Available online at www.sciencedirect.com
ScienceDirect
journal homepage: www.JournalofSurgicalResearch.com

Effects of rikkunshito, a kampo medicine, on quality of life after proximal gastrectomy

Shutaro Gunji, MD, Shugo Ueda, MD, PhD, Masahiro Yoshida, MD, Michiyuki Kanai, MD, PhD, Hiroaki Terajima, MD, PhD, and Arimichi Takabayashi, MD, PhD*

Department of Gastroenterological Surgery and Oncology, Tazuke Kofukai Medical Research Institute, Kitano Hospital, Osaka, Japan

ARTICLE INFO

Article history:
Received 15 January 2013
Received in revised form
18 May 2013
Accepted 5 June 2013
Available online 28 June 2013

Keywords:
Rikkunshito
Ghrelin
Gastrointestinal Symptom Rating Scale
Proximal gastrectomy
Postgastrectomy syndrome
quality of life

ABSTRACT

Background: The loss of the gastroesophageal junction after proximal gastrectomy (PG) induces various gastrointestinal symptoms, such as regurgitation, anorexia, and body weight loss, leading to impairment of the postoperative quality of life. In the present study, we investigated the long-term quality of life and the effects of rikkunshito, a traditional Japanese medicine (kampo), on the gastrointestinal symptoms and plasma ghrelin levels in patients with gastric cancer who had undergone PG.

Methods: Nineteen patients who had undergone PG> 6 mo before entry into the present study were enrolled. The plasma ghrelin levels, body weight, appetite, and Gastrointestinal Symptom Rating Scale (GSRS) scores were examined before and after the 4-wk administration of rikkunshito. A subgroup analysis was performed of patients showing a GSRS score of ≥ 2 before treatment, indicating the presence of gastrointestinal symptoms.

Results: The patients' body weight increased significantly after the administration of rikkunshito. Neither their appetite nor plasma acylated and deacylated ghrelin levels were significantly affected. In the subgroup analysis, the mean total GSRS score improved significantly from 2.6 ± 0.6 before the administration of rikkunshito to 1.9 ± 0.7 after administration because of the significant improvement in the subscale scores for abdominal pain, acid reflux, diarrhea, and constipation.

Conclusions: The long-term quality of life was well preserved in the patients who had undergone PG at our hospital. In the patients with a baseline GSRS score of ≥ 2, rikkunshito significantly improved the symptoms of postgastrectomy syndrome, and its effect was possibly independent of the plasma ghrelin levels.

1. Introduction

With the progress of endoscopic technology, a greater number of gastric cancer cases are being diagnosed at an early stage [1]. Total gastrectomy (TG) has been established as the standard surgery for advanced gastric cancer located in the cardia or the upper body of the stomach. However, proximal gastrectomy (PG) to maintain the reservoir function of the stomach is an optional surgical procedure for early stage gastric cancer or gastrointestinal stromal tumor in a proximal location, because metastasis in the distal perigastric lymph node is rare [2]. After PG, the loss of the lower esophageal

* *Corresponding author.* Department of Gastroenterological Surgery and Oncology, Tazuke Kofukai Medical Research Institute, Kitano Hospital, 2-4-20 Ohgimachi, Kita-ku, Osaka 530-8480, Japan. Tel.: +81 6 6312 8831; fax: +81 6 6312 8867.
E-mail address: shu-ueda@kitano-hp.or.jp (S. Ueda).
0022-4804/$ – see front matter © 2013 Elsevier Inc. All rights reserved.
http://dx.doi.org/10.1016/j.jss.2013.06.010

sphincter and the acute angle of His will lead to acid reflux, regurgitation, and anorexia, inducing weight loss and impairing postoperative quality of life (QOL) [3]. At Kitano Hospital, when the remnant stomach is large enough, an esophagogastric anastomosis with cardioplasty has been the standard procedure for reconstruction after PG; it maintains cardia function by forming a pseudo-fornix and pseudo-angle of His and thus improving postoperative QOL (Fig. 1) [4].

Operations on the stomach affect the secretion of various digestive hormones such as gastrin, motilin, vasoactive intestinal polypeptide, leptin, somatostatin, and ghrelin, resulting in impaired digestive function [5,6]. Ghrelin acts on the pituitary gland to enhance secretion of growth hormone [7] and on the hypothalamus to increase appetite [8]. Ghrelin is secreted mainly from the gastric endocrine X/A-like cells and, in part, from the duodenum, jejunum, and lung [8,9]. Among the gastric endocrine cells, X/A-like cells represent the second largest cell population (the largest being histamine-secreting enterochromaffin-like cells) [8]. The plasma ghrelin concentration decreases immediately after gastrectomy and recovers gradually thereafter; however, recovery has been poor after both TG and PG [6], because ghrelin-secreting X/A-like cells are abundant in the gastric fundus [8].

Rikkunshito (Tsumura, Tokyo, Japan), a traditional Japanese medicine (kampo) and a granular preparation of an herbal extract, was reported to improve gastric emptying in patients with functional dyspepsia [10,11] and in patients who underwent pylorus-preserving gastrectomy [12]. Recently, rikkunshito was reported to increase food intake and body weight in a rat anorexia model induced by administration of cisplatin. One of rikkunshito's mechanisms of action is said to enhance the secretion of acyl-ghrelin (i.e., the activated form of ghrelin) [13]; rikkunshito was also reported to improve symptoms in patients with functional dyspepsia, and the plasma ghrelin levels increased in these patients [14].

Although a previous study showed that plasma ghrelin levels decreased immediately after PG [6], it remains to be clarified whether rikkunshito affects ghrelin levels in the long term in postgastrectomy patients, because they lack the gastric fundus containing most of the ghrelin-secreting X/A cells. In the present study, we investigated the postoperative QOL of patients during long-term follow-up after PG and the effects of rikkunshito on postgastrectomy symptoms and plasma ghrelin levels in these patients.

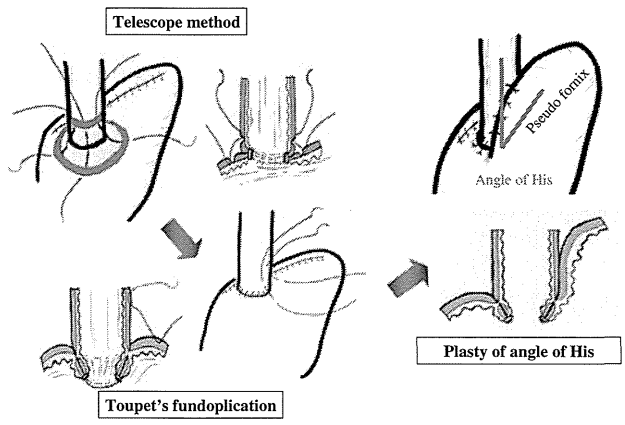

Fig. 1 – Illustration of cardioplasty after PG and esophagogastric anastomosis, using a telescope method combined with a Toupet fundoplication, forming a pseudo-fornix and pseudo-angle of His to maintain cardia function. (Color version of figure is available online.)

2. Methods

2.1. Patients

Of 90 patients with gastric cancer, including gastrointestinal stromal tumor, who had undergone PG at Tazuke Kofukai Medical Research Institute, Kitano Hospital from January 1992 to March 2009, 69 patients survived and could be followed up. Of these patients, 19, who met the following inclusion criteria, were enrolled in the present study: (1) age ≥20 but <80 y; (2) stage IA, IB, or II gastric cancer according to the International Union Against Cancer, 6th edition, TNM classification; (3) interval after surgery of ≥24 wk; and (4) grade 1 or greater anorexia according to the Common Terminology Criteria for Adverse Events, version 3.0. The exclusion criteria were (1) the presence of recurrent or metastatic cancer; (2) the presence of major organ damage, cardiac failure, or acute inflammatory disease; (3) difficulty in taking oral drugs; (4) female patients who were pregnant, desiring pregnancy, or breastfeeding; (5) a history of hypersensitivity to any kampo preparation; and (6) ineligibility judgment by the investigator. A QOL questionnaire survey on digestive symptoms, using the Gastrointestinal Symptom Rating Scale (GSRS), was administered to all the participants.

2.2. Study design

The present study was an open-label, prospective, single-arm study performed to investigate the long-term QOL of patients who underwent PG for early-stage gastric cancer >6 mo before the present study and to determine the pharmacologic effects, efficacy, and safety of rikkunshito in those patients.

Rikkunshito (Tsumura) is a granular preparation extracted with hot water of a mixture of eight crude drugs: *Atractylodis lanceae rhizoma, Ginseng radix, Pinelliae tuber, Hoelen, Zizyphi fructus, Aurantii nobilis pericarpium, Glycyrrhizae radix, and Zingiberis rhizoma* [13]. The patients were administered 2.5 g of rikkunshito 3 times daily before each meal for 4 wk. During treatment with rikkunshito, the patients were prohibited from using antiulcer agents such as proton pump inhibitors or gastrointestinal motility-enhancing agents such as metoclopramide or mosapride.

The primary endpoint was to evaluate whether rikkunshito improved the QOL and appetite of those patients; the method of evaluation has been described in the next section. The secondary endpoints were to evaluate the plasma concentration of both the active acylated and the inactive deacylated form of ghrelin, the ratio of acylated to deacylated ghrelin (A/D ratio), and the body weight. These parameters were measured before and after 4 wk of rikkunshito administration on the same day as the blood sampling.

The study was conducted according to the ethical guidelines for clinical studies in consideration of the patients' human rights and privacy. The institutional review board of

Kitano Hospital approved the protocol of the present study. All the patients received sufficient explanation about the study from the explanation and consent form approved by the institutional review board and provided written voluntary consent to participate in the present study.

2.3. *Measurement of plasma ghrelin levels*

The plasma samples were collected before breakfast (between 9:00 and 10:00 AM); they were promptly centrifuged at 4°C, and the supernatants were acidified with 1 mol/L HCl (1/10 volume). The plasma levels of the acylated and deacylated ghrelin were determined using the Active Ghrelin or Desacyl Ghrelin Enzyme-Linked Immunoassay Kit (Mitsubishi Kagaku Iatron, Tokyo, Japan) [15].

2.4. *Appetite evaluation using visual analog scale*

Visual analog scales (VAS) are an effective and reproducible tool for evaluating postoperative QOL [16–18]. Each patient's feeling of hunger, sensation of satiety or fullness, prospective food and beverage consumption, and the desire to eat and drink were scored on an anchored 100-mm VAS before and after the administration of rikkunshito. The scale ranged from "not at all" on the left end (0) to "extremely" on the right end (100); however, the subjects were unaware of the numbers. Each patient was instructed to mark, with a single vertical line, a point at which the length of the line matched their subjective sensation. All the VAS scores were provided on a separate form at each point and were collected immediately after they were completed.

2.5. *Gastrointestinal Symptom Rating Scale*

The gastrointestinal symptoms were evaluated using the GSRS [19]. GSRS is an inquiry table consisting of 15 items for evaluation of general gastrointestinal symptoms [20] (Table 1). Each was rated on a 7-point Likert scale from 1–7: no discomfort, minor, mild, moderate, moderately severe, severe, or very severe discomfort. Using a factor analysis, the 15 GSRS items were grouped into the following 5 categories: abdominal pain (upper abdominal pain, hunger pain, and nausea), reflux syndrome (heartburn and acid regurgitation), diarrhea syndrome (diarrhea, loose stools, and urgent need for defecation), indigestion syndrome (borborygmus, abdominal distension, eructation, and increased flatus), and constipation syndrome (constipation, hard stools, and a feeling of incomplete evacuation). The total score of the GSRS is the average of those five subscales: reflux symptoms, abdominal pain, indigestion, diarrhea, and constipation, ranging from 1–7, with greater scores representing more discomfort. If the score was $\geq$2, we judged that the patient showed significant active gastrointestinal symptoms.

2.6. *Subgroup analysis*

A subgroup analysis was performed of 10 patients who, before rikkunshito treatment, had a total GSRS score of $\geq$2, which was defined as uncomfortable gastrointestinal symptoms.

Table 1 – Gastrointestinal Symptom Rating Scale (GSRS) inquiry table.

Reflux symptoms (average score of 2 items)
Heartburn
Acid regurgitation
Abdominal pain (average score of 3 items)
Upper abdominal pain
Nausea
Hunger pains
Indigestion (average score of 4 items)
Borborygmus
Abdominal distension
Eructation
Increased flatus
Diarrhea (average score of 3 items)
Diarrhea
Loose stools
Urgent need for defecation
Constipation (average score of 3 items)
Constipation
Hard stools
Feeling of incomplete evacuation
Total symptoms = (reflux symptoms + abdominal pain + indigestion + diarrhea + constipation)/5

GSRS contains 15 items for evaluation of general gastrointestinal symptoms; each item was rated on a 7-point Likert scale, with 1 representing no discomfort and 7 representing very severe discomfort.

2.7. *Compliance, adverse events, safety, and tolerability*

Treatment compliance was defined as the percentage of the study drug used. A treatment compliance of >66.6% was considered feasible.

The safety and tolerability of rikkunshito were assessed by recording all adverse events and changes in hematologic and clinical laboratory variables. Any unfavorable or unintended signs were defined as adverse events, irrespective of whether they were considered to be causally related to rikkunshito.

2.8. *Statistical analysis*

The treatment response to rikkunshito was evaluated by the changes in body weight, the appetite VAS score, plasma ghrelin levels, and GSRS scores before and after treatment. Statistical analysis was performed using the Wilcoxon signed-rank test. $P < 0.05$ was considered statistically significant.

3. Results

3.1. *Patient characteristics*

The baseline characteristics of the 19 patients enrolled in the present study are listed in Table 2. The 19 patients included 16 men and 3 women, with an age range of 59–79 y (median age 73). The number of patients with International Union Against Cancer stage IA, IB, and II was 17, 1, and 1, respectively. Reconstruction was performed with esophagogastric anastomosis, double tract, and jejunal interposition in 17, 1, and 1 patient, respectively. The median interval from surgery to

Table 2 – Baseline patient characteristics (n = 19).

Characteristic	Value
Gender	
Male	16
Female	3
Age (y)	
Median	73
Range	59–79
International Union Against Cancer stage	
IA	17
IB	1
II	1
Reconstruction	
Esophagogastric anastomosis	17
Jejunal interposition	1
Double tract	1
Interval from surgery to study inclusion (y)	
Median	5.7
Range	0.5–16

study participation was 5.7 y (range 0.5–16). One female patient was excluded from the efficacy analysis, because she discontinued rikkunshito by her own decision.

3.2. *Changes in plasma ghrelin levels*

Figure 2 shows the changes in plasma acylated and deacylated ghrelin levels with rikkunshito treatment. The mean plasma level of acylated ghrelin before and after treatment was 7.67 and 7.61 fmol/L, respectively. The deacylated ghrelin level before and after treatment was 38.25 and 38.70 fmol/L, respectively. The A/D ratio before and after treatment was

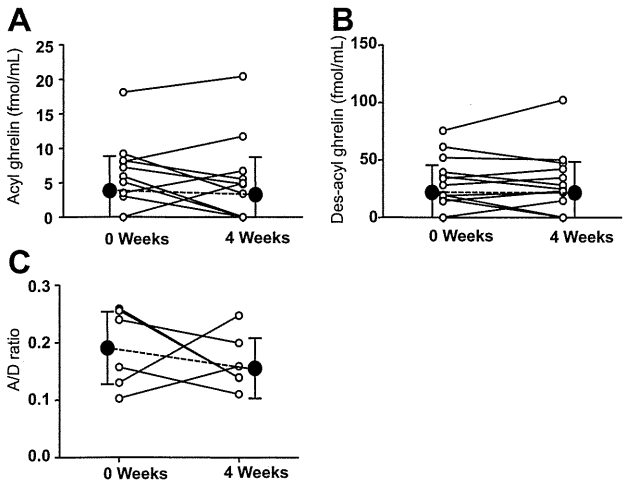

Fig. 2 – Individual results of acylated and deacylated ghrelin levels, before and after treatment with rikkunshito, in patients who underwent PG. (A) Plasma acylated ghrelin levels; (B) plasma deacylated ghrelin levels; (C) A/D ratio. Open circles indicate each patient's levels at each point; closed circles indicate average ghrelin levels or A/D ratios. No significant difference was found between before and 4 wk after treatment (Wilcoxon signed-rank test).

Table 3 – Change in body weight and appetite (VAS scores) and GSRS scores.

	At baseline (0 wk)	At study end (4 wk)	P value
Body weight (kg)	56.8 ± 7.7	57.2 ± 7.7	0.008
Appetite (VAS)	69.7 ± 16.3	68.7 ± 18.1	NS
GSRS total score	2.2 ± 0.7	2.1 ± 0.9	NS
Acid reflux symptoms	2.6 ± 1.2	2.2 ± 1.3	NS
Abdominal pain	1.8 ± 1.0	1.7 ± 0.9	NS
Dyspepsia-like symptoms	2.0 ± 0.6	2.3 ± 0.7	NS
Diarrhea symptoms	2.2 ± 1.1	2.1 ± 1.5	NS
Constipation symptoms	2.4 ± 0.7	2.4 ± 1.2	NS

NS = not significant.
Data are presented as average ± standard deviation.
GSRS scores ranged from 1 (no discomfort) to 7 (very severe discomfort); appetite (VAS) score ranged from 0 (not at all) to 100 (extremely).

0.21 and 0.16, respectively (P = 0.47). The results show no significant differences in plasma ghrelin levels from before to after treatment with rikkunshito.

3.3. *Changes in body weight, appetite, and gastrointestinal symptoms*

The patients' body weight increased significantly with the 4-wk treatment with rikkunshito; the average at baseline and after treatment was 56.8 and 57.2 kg, respectively (P = 0.008; Table 3). However, appetite, as assessed using the VAS, did not change significantly, with an average score before and after treatment of 69.7 and 68.7, respectively (Table 3). The average total GSRS score at baseline and after treatment was 2.2 and 2.1, respectively, showing no significant change in gastrointestinal symptoms (Table 3).

3.4. *Subgroup analysis of gastrointestinal symptoms using GSRS, body weight, and plasma ghrelin levels*

We analyzed the change in the subgroup of 10 patients with a baseline total GSRS score of ≥2, indicating bothersome symptoms. In this subgroup, 1 patient had undergone jejunal interposition, 1 had undergone double tract reconstruction, and the others had undergone esophagogastric anastomosis.

The total GSRS score for this subgroup had decreased significantly from 2.6 ± 0.6 at baseline to 1.9 ± 0.7 after the 4-wk treatment with rikkunshito (P = 0.002; Fig. 3). Among the GSRS subscale scores, the scores for abdominal pain, acid reflux, diarrhea, and constipation had improved significantly. However, no significant effect was seen for the indigestion symptoms.

The body weight did not change significantly; the average before and after treatment was 56.2 and 56.5 kg, respectively (P = 0.25). No significant differences were found in the plasma ghrelin levels or A/D ratios from before to after treatment (data not shown).

3.5. *Compliance and adverse events*

Of the 19 patients, 18 took the designated amount of rikkunshito during the study period. The rate of compliance was 95%, showing that it is feasible to take the medicine for 4 wk.

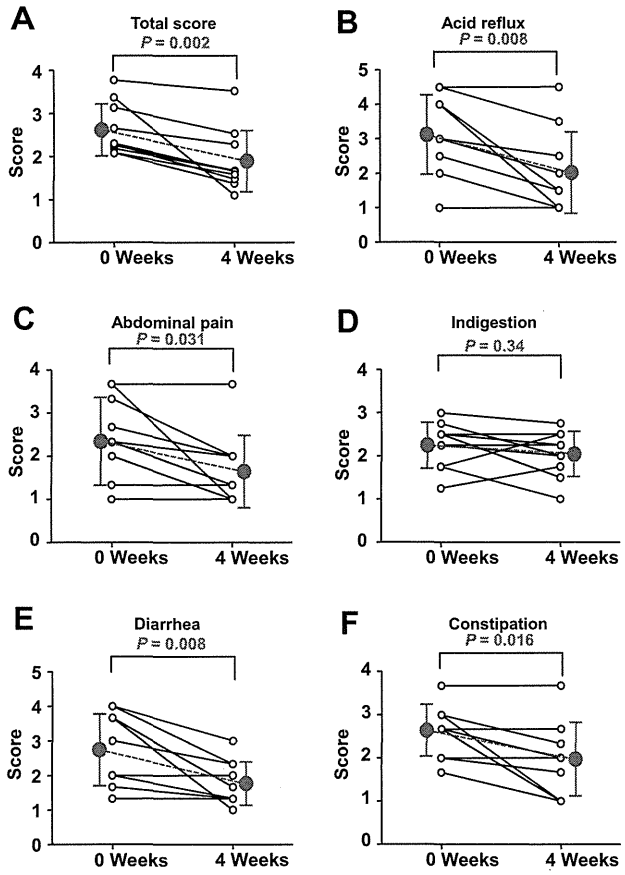

Fig. 3 – Subgroup analysis of gastrointestinal symptoms in patients with a baseline GSRS score of ≥2. Changes in total or subscale GSRS score were observed in 10 patients complaining of gastrointestinal symptoms. (A) Total score; (B) acid reflux symptom score; (C) abdominal pain score; (D) indigestion symptom score; (E) diarrhea symptom score; (F) constipation symptom score. Open circles indicate each patient's score at each point; closed circles indicate average scores of the patients. GSRS scores ranged from 1 (no discomfort) to 7 (very severe discomfort). P values with significant difference from before to 4 wk after treatment are shown (Wilcoxon signed-rank test).

No adverse events or reactions, such as impairment of liver function or allergic reactions, occurred throughout the observation period (data not shown).

4. Discussion

In the present prospective study, we investigated the effects of rikkunshito and QOL of patients who had undergone PG > 6 mo (median 5.7 y) before the present study. The average total GSRS score before treatment was 2.2, indicating that the QOL of many of the patients enrolled in the present study had not been impaired significantly by postgastrectomy syndrome (Table 3). Of the 19 enrolled patients, 17 had undergone reconstruction with an esophagogastric anastomosis and a cardioplasty forming a pseudo-fornix and pseudo-angle of His to maintain cardia function (Fig. 1). The reconstruction procedure we used to avoid gastroesophageal reflux seemed to keep patients relatively comfortable in the postgastrectomy state. The 4-wk administration of rikkunshito significantly increased the patients' body weight. Rikkunshito also significantly ameliorated postgastrectomy symptoms in a subgroup of symptomatic patients whose baseline GSRS score was ≥2. Rikkunshito seems to be more effective for patients with noticeable symptoms.

A previous report showed that 2 wk of rikkunshito administration increased the plasma ghrelin levels in healthy adults [15], suggesting that 4 wk of treatment with rikkunshito in the present study was a sufficient duration to investigate the efficacy of rikkunshito. However, treatment with rikkunshito did not affect the plasma acylated and deacylated ghrelin levels in our patients (Fig. 2). Ghrelin is mainly secreted from the gastric endocrine cells termed "X/A-like cells," which are mostly localized to the gastric fundus [8]. A previous study showed that plasma ghrelin levels decreased immediately after TG to 35% of those in healthy people [9]. Others have reported that low ghrelin levels persisted in the long term after TG, although the ghrelin levels in patients with distal gastrectomy gradually recovered [21]. Because of the loss of the cardiac fundus and thus many of the ghrelin-secreting X/A-like cells in the patients who had undergone PG, the ghrelin levels in the patients after PG declined similarly to those in patients who had undergone TG [6]. Therefore, it is possible that in the present study, rikkunshito did not affect the ghrelin levels in our patients receiving long-term follow-up after PG.

Rikkunshito has been known to enhance gastric emptying, motility, and adaptive relaxation, leading to its efficacy in the treatment of anorexia, reflux, and dyspepsia [10,11]. Hesperidin and L-arginine are the active ingredients of rikkunshito and contribute to facilitating gastric emptying, for which nitric oxide and the antagonistic action of the serotonin ($5\text{-}HT_3$) receptor pathway seem to be involved [22,23]. Therefore, the improvement in postgastrectomy symptoms by rikkunshito, especially in patients who had undergone PG, seems to be mediated by pathways other than ghrelin signaling.

The limitations of the present study were as follows. First, because our study was not a double-blind study, a placebo effect could not completely be excluded. Second, the number of patients was limited, because our study was conducted at a single institution and mainly included patients who had undergone the same surgical procedure. Therefore, if possible, we hope to extend the present study to other institutions and other surgical procedures for PG to investigate the effects of rikkunshito on those patients and their endocrine conditions.

5. Conclusions

The long-term QOL after PG was relatively well preserved in patients treated at our hospital. In patients who underwent PG > 6 mo before study inclusion, the 4-wk administration of rikkunshito significantly increased body weight. It also improved the QOL of symptomatic patients. The treatment did not affect the plasma ghrelin levels, suggesting that rikkunshito's mechanism of action for improving the patients' QOL after PG is independent of ghrelin signaling.

Acknowledgment

This study was supported by a grant from Tsumura & Co (gs1). We thank Naoko Tsuchiya, Chiharu Sadakane, and Ryouhei Inami for their help and advice with the present study.

REFERENCES

[1] Crew KD, Neugut AI. Epidemiology of gastric cancer. World J Gastroenterol 2006;12:354.
[2] Kitamura K, Yamaguchi T, Nishida S, et al. The operative indications for proximal gastrectomy in patients with gastric cancer in the upper third of the stomach. Surg Today 1997; 27:993.
[3] An JY, Youn HG, Choi MG, et al. The difficult choice between total and proximal gastrectomy in proximal early gastric cancer. Am J Surg 2008;196:587.
[4] Takabayashi A, Obama K. Esophago-gastric anastomosis with flatter valve and pinch cock after proximal gastrectomy. Shujutsu 2001;55:691. in Japanese.
[5] Yamashita Y, Hirai T, Toge T, et al. Adaptive gastrointestinal hormone changes after gastric resection. Dig Surg 1997;14:512.
[6] Jeon TY, Lee S, Kim HH, et al. Changes in plasma ghrelin concentration immediately after gastrectomy in patients with early gastric cancer. J Clin Endocrinol Metab 2004;89:5392.
[7] Kamegai J, Tamura H, Shimizu T, et al. Regulation of the ghrelin gene: growth hormone-releasing hormone upregulates ghrelin mRNA in the pituitary. Endocrinology 2001;142:4154.
[8] Date Y, Kojima M, Hosoda H, et al. Ghrelin, a novel growth hormone-releasing acylated peptide, is synthesized in a distinct endocrine cell type in the gastrointestinal tracts of rats and humans. Endocrinology 2000;141:4255.
[9] Ariyasu H, Takaya K, Tagami T, et al. Stomach is a major source of circulating ghrelin, and feeding state determines plasma ghrelin-like immunoreactivity levels in humans. J Clin Endocrinol Metab 2001;86:4753.
[10] Kusunoki H, Haruma K, Hata J, et al. Efficacy of rikkunshito, a traditional Japanese medicine (kampo), in treating functional dyspepsia. Intern Med 2010;49:2195.
[11] Tatsuta M, Iishi H. Effect of treatment with liu-jun-zi-tang (TJ-43) on gastric emptying and gastrointestinal symptoms in dyspeptic patients. Aliment Pharmacol Ther 1993;7:459.
[12] Takahashi T, Endo S, Nakajima K, et al. Effect of rikkunshito, a Chinese herbal medicine, on stasis in patients after pylorus-preserving gastrectomy. World J Surg 2009;33:296.
[13] Takeda H, Sadakane C, Hattori T, et al. Rikkunshito, an herbal medicine, suppresses cisplatin-induced anorexia in rats via 5-HT2 receptor antagonism. Gastroenterology 2008; 134:2004.
[14] Arai M, Matsumura T, Tsuchiya N, et al. Rikkunshito improves the symptoms in patients with functional dyspepsia, accompanied by an increase in the level of plasma ghrelin. Hepatogastroenterology 2012;59:62.
[15] Matsumura T, Arai M, Yonemitsu Y, et al. The traditional Japanese medicine rikkunshito increases the plasma level of ghrelin in humans and mice. J Gastroenterol 2010;45:300.
[16] Korolija D, Sauerland S, Wood-Dauphinee S, et al. Evaluation of quality of life after laparoscopic surgery: evidence-based guidelines of the European Association for Endoscopic Surgery. Surg Endosc 2004;18:879.
[17] Grant S, Aitchison T, Henderson E, et al. A comparison of the reproducibility and the sensitivity to change of visual analogue scales, Borg scales, and Likert scales in normal subjects during submaximal exercise. Chest 1999;116:1208.
[18] Barczynski M, Herman RM. A prospective randomized trial on comparison of low-pressure (LP) and standard-pressure (SP) pneumoperitoneum for laparoscopic cholecystectomy. Surg Endosc 2003;17:533.
[19] Svedlund J, Sjodin I, Dotevall G. GSRS—a clinical rating scale for gastrointestinal symptoms in patients with irritable bowel syndrome and peptic ulcer disease. Dig Dis Sci 1988; 33:129.
[20] Revicki DA, Wood M, Wiklund I, et al. Reliability and validity of the Gastrointestinal Symptom Rating Scale in patients with gastroesophageal reflux disease. Qual Life Res 1998;7:75.
[21] Takachi K, Doki Y, Ishikawa O, et al. Postoperative ghrelin levels and delayed recovery from body weight loss after distal or total gastrectomy. J Surg Res 2006;130:1.
[22] Kido T, Nakai Y, Kase Y, et al. Effects of rikkunshi-to, a traditional Japanese medicine, on the delay of gastric emptying induced by N(G)-nitro-L-arginine. J Pharmacol Sci 2005;98:161.
[23] Tominaga K, Kido T, Ochi M, et al. The traditional Japanese medicine rikkunshito promotes gastric emptying via the antagonistic action of the 5-HT(3) receptor pathway in rats. Evid Based Complement Alternat Med 2011;2011:248481.

Journal of proteome research

Perspective

pubs.acs.org/jpr

Integrated View of the Human Chromosome X-centric Proteome Project

Tadashi Yamamoto,*[,†] Keiichi Nakayama,[‡] Hisashi Hirano,[§] Takeshi Tomonaga,[∥] Yasushi Ishihama,[⊥] Tetsushi Yamada,[#] Tadashi Kondo,[#] Yoshio Kodera,[□] Yuichi Sato,[□] Norie Araki,[¶] Hiroshi Mamitsuka,[○] and Naoki Goshima[●]

[†]Institute of Nephrology, Graduate School of Medical and Dental Sciences, Niigata, Japan

[‡]Medical Institute of Bioregulation, Kyushu University, Kyushu, Japan

[§]Graduate School of Nanobioscience, Yokohama City University, Yokohama, Japan

[∥]Laboratory of Proteome Research, National Institute of Biomedical Innovation, Ibaraki, Japan

[⊥]Graduate School of Pharmaceutical Sciences, Kyoto University, Kyoto, Japan

[#]National Cancer Center Research Institute, Tokyo, Japan

[□]Kitasato University, Kanagawa, Japan

[¶]Graduate School of Medical Sciences, Kumamoto University, Kumamoto, Japan

[○]Bioinformatics Center, Institute for Chemical Research, Kyoto University, Uji, Japan

[●]National Institute of Advanced Industrial Science and Technology (AIST), Tokyo, Japan

ABSTRACT: This article introduces how the human chromosome X-centric proteome project is carried out by the Japan Chromosome X Project Consortium. The inactivation of one of two chromosomes in female mammals and accumulation of genes related to neural/immune systems/tumor/testis are characteristic of chromosome X. In this Chromosome X Project, information on proteins translated from genes on chromosome X is collected by both mass spectrometry- and antibody-based proteomics. Information on the following resources is also provided: antibodies to proteins translated and full-length cDNAs transcripted from the chromosome X genes for recombinant proteins. The consortium aims to provide the following tools to search useful antibodies in the literature (Antibody Ranker), to find gene expression sites in microarray databases (Transcript Localizer) and to do advanced MRM analysis (information-based MRM).

KEYWORDS: *chromosome X, mass spectrometry, antibody, MRM*

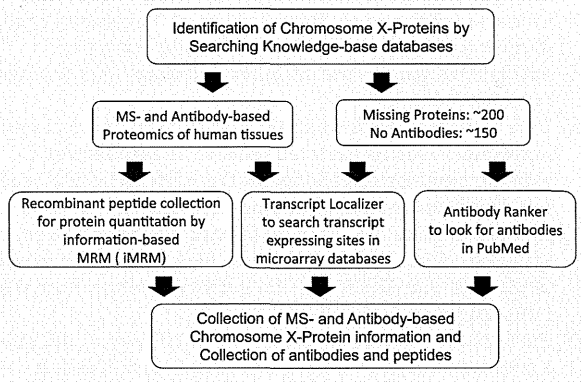

■ INTRODUCTION

Chromosome X is one of the two sex-determining chromosomes (the other is the Y chromosome) in many animal species, including mammals, and is found in both males and females. This chromosome has the following characteristics, which are not found in other chromosomes: presence of sex-determining genes such as androgen receptor gene, inactivation of one of two chromosomes (X-inactivation), a large number of genes associated with human hereditary diseases, and significant accumulation of genes for networks in neuronal, immune and tumor-related systems.

The Japanese Proteomics Society (JHUPO) was chosen to participate in the Chromosome-centric Human Proteome Project and was asked to be in charge of chromosome X. The Japan Chromosome X Project Consortium (JCXPC) was organized to complete the project by collecting information and resources of all proteins translated from genes located on chromosome X (chromosome X-proteins). Knowledge of the human chromosome X-proteins and the current activities and aims of the chromosome X project are briefly described.

■ KNOWLEDGE OF HUMAN CHROMOSOME X

1. Characteristics

The human chromosome X spans about 153 million base pairs (4.94%) out of 3100 million base pairs of total human DNA length. The number of genes on chromosome X is presumed to be 888 genes (4.37%) out of total human genes of 20300.[1] The other sex-determining chromosome, Y chromosome, has only 68 genes and one of these genes, named SRY (Sex-determining

Special Issue: Chromosome-centric Human Proteome Project

Received: September 5, 2012
Published: December 21, 2012

Table 1. Summary of Genes and Proteins on Human Chromosome X

identification level	database	identified/total	%	URL
Transcript	neXtProt	823/874	94.2%	http://www.nextprot.org
neXtProt	neXtProt	615/874	70.4%	http://www.proteinatlas.org/
	Peptide Atlas	396/874	45.3%	http://www.peptideatlas.org
	SRM Atlas	~19000/ ~20300	93.6%[a]	http://www.srmatlas.org
	GPM DB	657/862	76.2%	http://www.thegpm.org
Protein by Antibody	HPA	495/841	55.7%	http://www.proteinatlas.org
	Antibodypedia	722/874	82.6%	http://www.antibodypedia.com
Disorders associated[b]	neXtProt	195/874	22.3%	
	OMIM Gene Map	305/874	34.9%	http://omim.org/geneMap
	Genetics Home Reference	107/874	12.2%	http://ghr.nlm.nih.gov/chromosome/X/show/Conditions

[a]Estimated based on all genes. [b]Including Dominant X-linked diseases (related gene): Vitamin D resistant rickets (X-linked hypophosphatemia, PHEX), Rett syndrome (MECP2), Fragile X syndrome (FMR1), Alport syndrome (COL4A5), etc. X-linked recessive inheritance: Color blindness (OPN1MW, OPN1LW), Hemophilia (F8, F9), Duchenne muscular dystrophy (DMD), X-linked agammaglobulinemia (BTK), Fabry disease (GLA), etc.

Region on the Y chromosome), determines male by inducing and developing the testis to produce a male hormone, androgen. On the chromosome X only a few of the 888 genes directly play a role in sex determination. One is the gene encoding androgen receptor on the chromosome X, indicating the importance of chromosome X in males and suggesting a cross-communication between chromosomes X and Y and also the significance of the androgen receptor in females.

Besides the sex-determining genes, genes in the neural system are uniquely clustered on chromosome X: NLGN3 (Neuroligin-3), NLGN4X (Neuroligin-4, X-linked), OPHN1 (Oligophrenin-1), PAK3 (Serine/threonine-protein kinase), FMR1 (fragile X mental retardation 1), MAG (myelin associated glycoprotein) and others. Proteins translated from these genes are essential for interaction or communication of neurons and are presumed to relate to the intelligence.[2] The important role of the X chromosome in brain function is also evident from the prevalence of X-linked forms of mental retardation.

The accumulation of immune system-related genes to chromosome X also attracts attention. CD40L (CD40 ligand), IL2RG (Cytokine receptor common subunit gamma), BTK (Tyrosine-protein kinase), F8 (Coagulation factor VIII), and F9 (Coagulation factor IX) are example of chromosome X genes that are involved in the immune system and coagulation system.[3]

The inactivation of chromosome X is a process by which one of the two copies of chromosome X in females is inactivated. The inactive X chromosome is transcriptionally silenced to form an inactive structure called heterochromatin. The choice of which X chromosome is inactivated is randomly occurring in each cell in mammals. The X-inactivation center on the X chromosome, which is essential to cause X-inactivation, contains four nontranslated RNA genes, Xist, Tsix, Jpx and Ftx, which are involved in X-inactivation.[4,5]

2. Human Chromosome X-Proteins Identified by Mass Spectrometry (MS)

Information of genes on chromosome X and the proteins encoded by the genes has been collected in several databases (Table 1). In the neXtProt database (http://www.nextprot.org), 874 genes are presumed on chromosome X.[1] Among them, 823 (94.2%) genes have been identified at the transcript level and 615 (70.4%) genes have been demonstrated at the protein level by proteomics. In the other proteome databases, Peptide Atlas and GPM DB (Global Proteome Machine database), 45.3 and 75.2%, respectively, of the genes on chromosome X are identified as proteins. However, these data indicate that more than 200 genes on chromosome X are still unclear whether they translate proteins or not. These unclear proteins are further confirmed by MS and immunohistochemistry using antibodies in this project.

3. Proteomes Identified by Antibody-based Methods

Collection and validation of antibodies against human proteins are progressing by Human Protein Atlas project.[6] By using antibodies, localization of 495 (56.6%) chromosome X-proteins has been examined at cellular and subcellular levels in human body.

The Antibodypedia is a Web site providing datasheets of antibodies against human proteins from antibody providers (http://www.antibodypedia.com). In this collection, datasheets of antibodies against 722 (82.6%) chromosome X-proteins are currently shown although these antibodies have not always been well-characterized in the specificity or reactivity to the proteins for immunolocalization. The Chromosome X Project Consortium members will collect significant evidence of the presence or localization of the chromosome X-proteins from the literature or from their own research.

4. Diseases Associated with Chromosome X

A large number of genes (195 in the neXtProt database) in chromosome X have been demonstrated to associate with genetic disorders and hereditary diseases in humans (Table 1). One of the reasons is only one copy of chromosome X is active both in males (XY) and females (XX) (X-inactivation), resulting in prevalence of X-linked hereditary diseases.

It is estimated that about 10% of the genes (99 genes) encoded by the X chromosome are associated with a family of "CT antigen (cancer-testis antigen)" genes, which encode for markers found in both cancer cells as well as in the human testis (MAGE, GAGE, SSX, SPANX or other CT gene families).[7]

THE JAPAN CHROMOSOME X PROJECT

1. Selection of Tissues and Organs

Since preference in expression of chromosome X genes in neural and immune systems and the tissues (neural and immune systems or cancers and testis) has been demonstrated as described above, it is presumed that expression of chromosome X-proteins is also different among organs or tissues. Therefore, expression of chromosome X-proteins were searched in the kidney, brain, ovary and testis in the Human

dx.doi.org/10.1021/pr300844p | J. Proteome Res. 2013, 12, 58−61

Protein Atlas. As shown in Table 2, there was no significant preference in the expression among the organs. Therefore, the

Table 2. Identification of Chromosome X-Proteins in the Human Protein Atlas[a]

		immunohistochemistry	
	antibodies used	strong (%)	weak (%)
Placenta	627	148 (23.6)	490 (78.1)
Kidney	900	149 (16.6)	654 (72.7)
Ovary	1180	160 (13.6)	825 (69.9)
Testis	1032	224 (21.7)	821 (79.6)
Brain	1112	159 (14.3)	776 (69.8)

[a]Placenta, kidney, ovary, testis and brain tissues were examined by immunohistochemistry using antibodies in the Human Protein Atlas (http:www.proteinatlas.org/). Numbers of antibodies used, stained the tissues strongly or more than weakly are shown (%).

Japan chromosome X project consortium preliminarily chose kidney, ovary, and breast as target sample tissues to look for chromosome X-proteins, which had not been well-identified yet because these organs had not been analyzed by other chromosome projects and our project members had already analyzed the proteomes of these organs more or less.

2. Collection of Protein Existence by MS

With informed consent, human kidney, ovary, breast tissues were obtained from patients when these organs or tissues were surgically removed for treatment of cancers. Kidneys were separated into cortex, medulla and glomerulus.[8] More fine structured (proximal tubule, distal tubule, collecting duct, and others) kidney sections were microdissected from kidney sections by laser microdissection system for deeper and more comprehensive MS analysis of kidney nephron parts. Other organs are also considered for such in depth MS analysis.

Members of the Japan Chromosome X Project are interested in MS analysis of cancers[9−12] and biofluids[13,14] for biomarker discovery and understanding of pathophysiology of cancers. Other members are also focusing on analysis of protein modification such as phosphorylation or glycosylation and collect MS evidence of post-translational modifications of chromosome X-proteins in the target organs and others.[15]

Another approach to find possible tissue or organ sites was carried out to develop a search engine ("Transcript Localizer") to look at human microarray databases and to pick up sites where missing or unclear chromosome X genes are detected.

3. Collection of Protein Localization by Antibodies

Cellular localization of proteins, which would first be identified by MS in the target organs, was secondarily searched in the Human Protein Atlas database and the immunohistochemistry images were retrieved to combine to the data obtained by MS-based proteomics. A prototype of the human kidney proteome database has been opened to the public at the Web site of the HUPO Human Kidney and Urine Proteome Project (HKUPP) Initiative (www.hkupp.org/). The members of the chromosome X project also examined localization of MS-identified proteins in the target organs by immunohistochemistry to confirm the Human Protein Atlas data and the MS identification results. Our consortium will collect information on antibodies to the proteins, which are not provided by the Human Protein Atlas project, by searching in the Antibodypedia.

We are also developing an antibody search engine tool that looks for antibodies in open free access articles in the PubMed database and picks up antibodies to human proteins and collects the following information: name of companies providing antibodies and images obtained by the antibodies. Several different antibodies to one human protein were used in the past studies and the search engine collects information of all of these antibodies and will demonstrate antibody information in a rank order of number of articles in which the same antibody was used. This informs us which antibody is mostly used for a human protein in a community of scientists. Therefore, the tool was named "Antibody Ranker". We believe this tool provides valuable information for researchers who are looking for antibodies for human proteins. Efficiency of the Antibody Ranker is also validated by selecting antibodies for immunohistochemistry in the chromosome X project.

4. Resources and Tools Developed from the Chromosome X Project

The Human Gene and Protein Database (HGPD; http://www.HGPD.jp/) launched in 2008 is a unique resource storing 43249 human Gateway entry clones constructed from the open reading frames (ORFs) of full-length human cDNA, which is the largest in the world.[16] Since the set of these clones are used for recombinant human protein synthesis by the wheat germ cell-free protein synthesis system, this resource is named the Human Proteome Expression Resource (HuPEX).[17] The recombinant protein resource has covered more than 85% of human proteins encoded by 20300 genes.

All synthesized proteins (approx. 18000) have been intensively analyzed by MS after trypsinization and MS/MS information of individual peptides from the proteins has been collected as a database for selection of peptides and MRM (multiple reaction monitoring) transitions. This provides us information to select peptides and MS/MS transitions for MRM (information-based MRM, iMRM) and also resources of reference peptides for quantitation of proteins in the target tissues.

■ CONCLUSION

Current status and future plans of the Japan human chromosome X project are summarized in Figure 1 .. Collaboration and cooperation with other chromosome

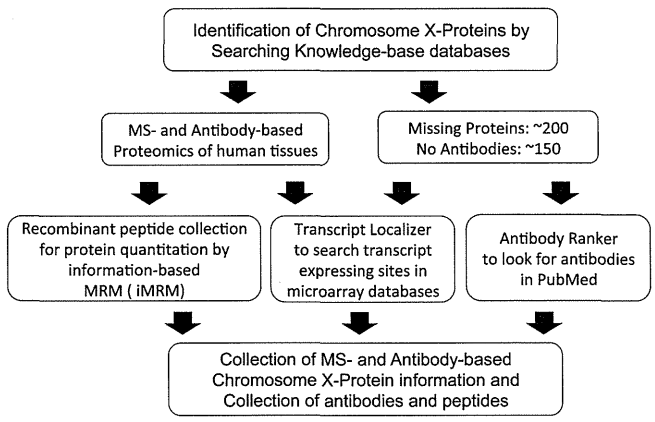

Figure 1. Workflow of Japan Chromosome X Project. Shown here is a strategy from basic collection of knowledge-base proteomics data to final completion of chromosome X proteome data and resource collection done by Japan Chromosome X Project Consortium.

dx.doi.org/10.1021/pr300844p | J. Proteome Res. 2013, 12, 58−61

projects in the Chromosome-centric Human Proteome Project, especially chromosome Y and with other Biology/Disease Human Proteome projects, need to be facilitated to complete the Human Proteome Project.

AUTHOR INFORMATION

Corresponding Author

*E-mail: tdsymmt@med.niigata-u.ac.jp. Tel: +81-25-227-2151. Fax: +81-25-227-0768.

Notes

The authors declare no competing financial interest.

ACKNOWLEDGMENTS

This study was supported by a Grant-in-Aid for Scientific Research (B) to T.Y. ((21390262) from Japan Society for Promotion of Science and by a Grant-in-Aid for Strategic Research Project to T.Y. (500460) from Ministry of Education, Culture, Sports, Science and Technology, Japan and by a Grant-in-Aid for Diabetic Nephropathy and Nephrosclerosis Research from the Ministry of Health, Labor and Welfare of Japan.

REFERENCES

(1) Lane, L.; Argoud-Puy, G.; Britan, A.; Cusin, I.; Duek, P. D; Evalet, O.; Gateau, A.; Gaudet, P.; Gleizes, A.; Masselot, A.; Zwahlen, C.; Bairoch, A. neXtProt: a knowledge platform for human proteins. *Nucleic Acids Res.* **2011**, *40*, D76−83.

(2) Nguyen, D. K; Disteche, C. M. High expression of the mammalian X chromosome in brain. *Brain Res.* **2006**, *1126*, 46−9.

(3) Libert, C.; Dejager, L.; Pinheiro, I. The X chromosome in immune functions: when a chromosome makes the difference. *Nat. Rev. Immunol.* **2010**, *10*, 594−604.

(4) Brockdorff, N. Chromosome silencing mechanisms in X-chromosome inactivation: unknown unknowns. *Development* **2011**, *138*, 5057−65.

(5) Reinius, B.; Shi, C.; Hengshuo, L.; Sandhu, K. S; Radomska, K. J; et al. Female-biased expression of long non-coding RNAs in domains that escape X-inactivation in mouse. *BMC Genomics* **2010**, *11*, 614.

(6) Uhlen, M.; Oksvold, P.; Fagerberg, L.; Lundberg, E.; Jonasson, K.; Forsberg, M.; Zwahlen, M.; Kampf, C.; Wester, K.; Hober, S.; Wernerus, H.; Björling, L.; Ponten, F. Towards a knowledge-based Human Protein Atlas. *Nat. Biotechnol.* **2010**, *28*, 1248−50.

(7) Ross, M.; Grafham, D. V; Coffey, A. J; Scherer, S.; McLay, K.; et al. The DNA sequence of the human X chromosome. *Nature* **2005**, *434*, 325−37.

(8) Miyamoto, M.; Yoshida, Y.; Taguchi, I.; Nagasaka, Y.; Tasaki, M.; et al. In-depth proteomic profiling of the normal human kidney glomerulus using two-dimensional protein prefractionation in combination with liquid chromatography-tandem mass spectrometry. *J Proteome Res.* **2007**, *6*, 3680−90.

(9) Masuishi, Y.; Arakawa, N.; Kawasaki, H.; Miyagi, E.; Hirahara, F.; Hirano, H.. Wild-type p53 enhances annexin IV gene expression in ovarian clear cell adenocarcinoma. *FEBS J.* **2011**, *27*, 1470−83.

(10) Muraoka, S.; Kume, H.; Watanabe, S.; Adachi, J.; Kuwano, M.; et al. Strategy for SRM-based verification of biomarker candidates discovered by iTRAQ method in limited breast cancer tissue samples. *J. Proteome Res.* **2012**, *11*, 4201−10.

(11) Ono, M.; Kamita, M.; Murakoshi, Y.; Matsubara, J.; Honda, K.; et al. Biomarker discovery of pancreatic and gastrointestinal cancer by 2DICAL: 2-dimensional image-converted analysis of liquid chromatography and mass spectrometry. *Int. J. Proteomics.* **2012**, *2012*, 897412.

(12) Sugihara, Y.; Taniguchi, H.; Kushima, R.; Tsuda, H.; Kubota, D.; et al. Proteomic-based identification of the APC-binding protein EB1 as a candidate of novel tissue biomarker and therapeutic target for colorectal cancer. *J. Proteomics* **2012**, *75*, 5342−55.

(13) Kawashima, Y.; Fukutomi, T.; Tomonaga, T.; Takahashi, H.; Nomura, F.; Maeda, T.; Kodera, Y. High-yield peptide-extraction method for the discovery of subnanomolar biomarkers from small serum samples. *J. Proteome Res.* **2010**, *9*, 1694−705.

(14) Kobayashi, M.; Matsumoto, T.; Ryuge, S.; Yanagita, K.; Nagashio, R.; et al. CAXII Is a sero-diagnostic marker for lung cancer. *PLoS One* **2012**, *7*, e33952.

(15) Imamura, H.; Wakabayashi, M.; Ishihama, Y. Analytical strategies for shotgun phosphoproteomics: status and prospects. *Semin. Cell Dev. Biol.* **2012**, *23*, 836−42.

(16) Goshima, N.; Kawamura, Y.; Fukumoto, A.; Miura, A.; Honma, R.; et al. Human protein factory for converting the transcriptome into an in vitro−expressed proteome. *Nat. Methods* **2008**, *5*, 1011−7.

(17) Maruyama, Y.; Kawamura, Y.; Nishikawa, T.; Isogai, T.; Nomura, N.; Goshima, N. HGPD: Human Gene and Protein Database, 2012 update. *Nucleic Acids Res.* **2012**, *40*, D924−9.

Hindawi Publishing Corporation
BioMed Research International
Volume 2013, Article ID 134813, 10 pages
http://dx.doi.org/10.1155/2013/134813

Hindawi

Research Article

An Active C-Terminally Truncated Form of Ca^{2+}/Calmodulin-Dependent Protein Kinase Phosphatase-N (CaMKP-N/PPM1E)

Atsuhiko Ishida,[1] Kumiko Tsumura,[1] Megu Oue,[1] Yasuhiro Takenaka,[2] Yasushi Shigeri,[2] Naoki Goshima,[2] Yasuhiro Ishihara,[1] Tetsuo Hirano,[1] Hiromi Baba,[3] Noriyuki Sueyoshi,[3] Isamu Kameshita,[3] and Takeshi Yamazaki[1]

[1] *Laboratory of Molecular Brain Science, Graduate School of Integrated Arts and Sciences, Hiroshima University, Higashi-Hiroshima 739-8521, Japan*
[2] *National Institute of Advanced Industrial Science and Technology, Ikeda, Osaka 563-8577, Japan*
[3] *Department of Life Sciences, Faculty of Agriculture, Kagawa University, Kagawa 761-0795, Japan*

Correspondence should be addressed to Atsuhiko Ishida; aishida@hiroshima-u.ac.jp

Received 5 April 2013; Revised 10 July 2013; Accepted 12 July 2013

Academic Editor: Y. George Zheng

Ca^{2+}/calmodulin-dependent protein kinase phosphatase (CaMKP/PPM1F) and its nuclear homolog CaMKP-N (PPM1E) are Ser/Thr protein phosphatases that belong to the PPM family. CaMKP-N is expressed in the brain and undergoes proteolytic processing to yield a C-terminally truncated form. The physiological significance of this processing, however, is not fully understood. Using a wheat-embryo cell-free protein expression system, we prepared human CaMKP-N (hCaMKP-N(WT)) and the truncated form, hCaMKP-N(1–559), to compare their enzymatic properties using a phosphopeptide substrate. The hCaMKP-N(1–559) exhibited a much higher V_{max} value than the hCaMKP-N(WT) did, suggesting that the processing may be a regulatory mechanism to generate a more active species. The active form, hCaMKP-N(1–559), showed Mn^{2+} or Mg^{2+}-dependent phosphatase activity with a strong preference for phospho-Thr residues and was severely inhibited by NaF, but not by okadaic acid, calyculin A, or 1-amino-8-naphthol-2,4-disulfonic acid, a specific inhibitor of CaMKP. It could bind to postsynaptic density and dephosphorylate the autophosphorylated Ca^{2+}/calmodulin-dependent protein kinase II. Furthermore, it was inactivated by H_2O_2 treatment, and the inactivation was completely reversed by treatment with DTT, implying that this process is reversibly regulated by oxidation/reduction. The truncated CaMKP-N may play an important physiological role in neuronal cells.

1. Introduction

Ca^{2+}/calmodulin-dependent protein kinase phosphatase (CaMKP/PPM1F/POPX2) was first identified in rat brain as a unique protein phosphatase that specifically dephosphorylates and regulates multifunctional CaMKs, including CaMKI, II, and IV [1–4]. Thereafter, another protein phosphatase with 52% identity in the catalytic domain to human CaMKP was found in the human cDNA databases (Figure 1(a)). When the cDNA was expressed in COS cells, the phosphatase encoded by the cDNA was localized to the nucleus, in contrast to CaMKP, which was exclusively found in the cytosol. Therefore, we named the enzyme CaMKP-N for its localization in the nucleus [5]. Subsequently, other groups named this enzyme POPX1 [6] or PPM1E [7] and reported that it is involved in the negative regulation of the p21-activated protein kinase [6] and the 5′-AMP-activated protein kinase [7]. Gene knockdown experiments for zebrafish CaMKP-N (zCaMKP-N) using morpholino-based antisense oligonucleotides indicated that CaMKP-N is essential for the early development of the brain and spinal cord in zebrafish [8].

We also showed that the proteolytic processing of zCaMKP-N plays a critical role in the regulation of its catalytic activity, subcellular localization, and substrate targeting [9]. In accordance with these results, Kitani et al.

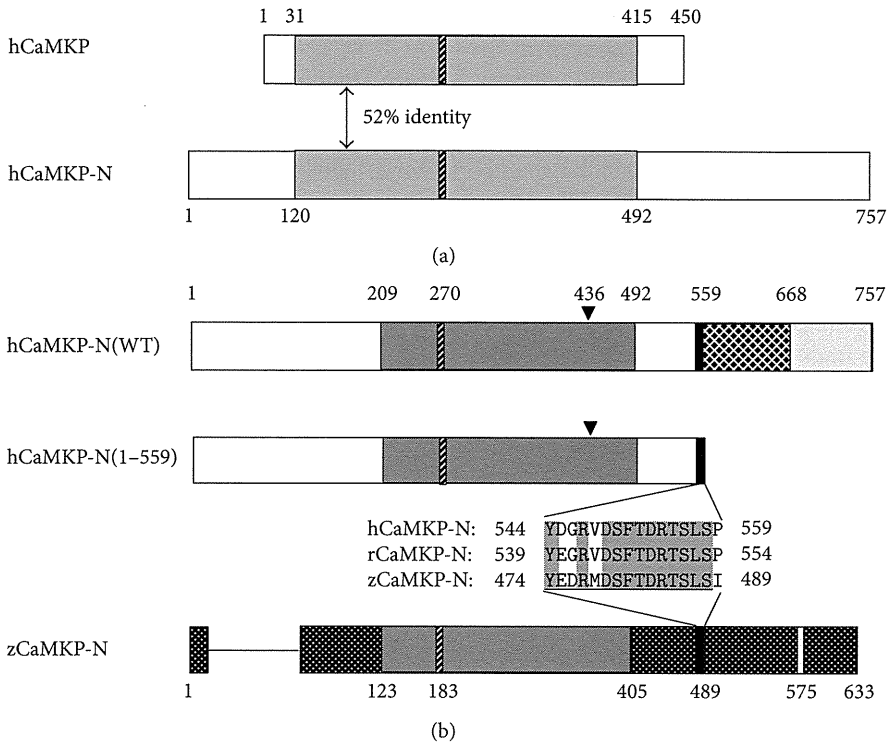

FIGURE 1: Schematic representation of hCaMKP, hCaMKP-N(WT), hCaMKP-N(1–559), and zCaMKP-N. (a) Comparison of the primary structure of hCaMKP-N with that of hCaMKP. The regions that show significant homology are shown in grey. (b) Domain structures of hCaMKP-N(WT), hCaMKP-N(1–559), and z-CaMKP-N. Catalytic domains are shown in dark grey, and the hatched bars within them indicate the PP2C motif that is characteristic of PPM family phosphatases. Black bars show the antibody recognition site. In hCaMKP-N, the recognition site is located just to the N-terminal side of the putative processing site. The amino acid sequences of the antibody recognition site in human, rat, and zebrafish CaMKP-N are also indicated. Underline shows the amino acid sequence used for generating the anti-CaMKP-N antibody. Closed arrowheads show the position of Cys436, which may be responsible for redox regulation of the phosphatase activity (see text). It has been reported that two nuclear localization signals are located in the region that is C-terminal side to Arg668 on hCaMKP-N (shown in light grey). The 575–587 region of zCaMKP-N reportedly functions as a nuclear localization signal (shown in light grey) [8]. The amino acid residue numbers of the respective phosphatases are also shown.

[10] suggested that the majority of CaMKP-N undergoes proteolytic processing to generate a 90 kDa fragment in rat brain that is localized to the cytosol. Since the amino acid sequence homology between zCaMKP-N and human CaMKP-N (hCaMKP-N) is only 48% and the molecular size of zCaMKP-N is much smaller than the size of hCaMKP-N (by more than 100 amino acid residues, Figure 1(b)), it is difficult to predict, on the basis of sequence homology, whether the 90 kDa fragment is a mammalian counterpart for the active fragment of zCaMKP-N that is generated by proteolytic processing in zebrafish. It is clinically significant to explore the enzymatic properties of hCaMKP-N, which may provide a molecular basis for drug development because CaMKP-N has been suggested to regulate the 5′-AMP-activated protein kinase involved in the pathogenesis of diabetes [7]. Unfortunately, difficulty in preparing hCaMKP-N in a sufficient purity and quantity has hampered the biochemical characterization of this enzyme. Our initial attempt to obtain pure full-length hCaMKP-N using transfected Sf9 cells failed due to proteolysis during the expression and purification. We performed only a preliminary characterization of hCaMKP-N using a mixed preparation that contained both full-length hCaMKP-N and its truncated fragment, which was generated during the preparation [5]. Therefore, no information has been available about the enzymatic properties and the physiological importance of each species of hCaMKP-N.

In this study, we utilized a wheat-embryo cell-free protein expression system to separately prepare full-length hCaMKP-N and hCaMKP-N(1–559), a human counterpart to the 90 kDa truncated fragment found in the rat brain. Using these preparations, we compared the kinetic properties of full-length hCaMKP-N and the truncated fragment, and we found that the truncated fragment had much higher phosphatase activity than the full-length form. We also examined the enzymatic properties of the truncated hCaMKP-N, which had not been characterized in detail, and discussed the physiological importance of the processing.

2. Materials and Methods

2.1. Materials. The phosphopeptides, pp2 (MHRQET**(p)**VDC), pp4 (MHRQES**(p)**VDC), pp6 (MHRQEY**(p)**VDC), and pp10 (YGGMHRQET**(p)**VDC), were synthesized using a Shimadzu PSSM-8 automated peptide synthesizer and

purified by reverse-phase HPLC on a C_{18} column [5, 11]. The identity and purity of the peptides were confirmed by time-of-flight mass spectrometry. The postsynaptic density (PSD) fraction was purified from rat cerebral cortex as described by Sahyoun et al. [12]. The anti-CaMKP-N antibody was obtained as previously described [8]. Monoclonal anti-CaMKIIα (MAb CBα-2) was purchased from Life Technologies. The anti-active CaMKII was from Promega. The biotin-conjugated rabbit anti-mouse IgG was obtained from ZYMED. The anti-rabbit Ig, biotinylated species-specific antibody, streptavidin-conjugated horseradish peroxidase, and the Ni^{2+}-Sepharose high-performance resin were from GE Healthcare. An enhanced chemiluminescence detection agent, SuperSignal West Femto Maximum Sensitivity Substrate, was from Thermo Scientific. DNase-free RNase was from Boeringer Mannheim. Hydrogen peroxide, Quick CBB, and okadaic acid were purchased from Wako Pure Chemical Industries, and the 1-amino-8-naphthol-2,4-disulfonic acid (ANDS) was from Tokyo Chemical Industry. Calyculin A was from Millipore/Upstate. All other agents were obtained from Nacalai Tesque or Sigma-Aldrich.

2.2. Construction of Plasmids. The pEU-E01-CaMKPN vector, which encodes the wild type (WT) hCaMKP-N with an N-terminal 6x His tag, was prepared as described in the following. The following primers were used for PCR: CaMKPN His-UP1 (5′-GGA TAT CTA TGT CGT ACT ACC ATC ACC ATC ACC ATC ACG CCG GCT GCA TCC CTG AGG AGA A-3′) with an *Eco*RV site (underlined) and CaMKPN LP1 (5′-GGT CGA CTT ATT CTA TTT TAT AGC TCC AAG GAA GAT-3′) with a *Sal*I site (underlined). The PCR was performed in a PTC-200 Thermal Cycler (MJ Research) for 20 cycles, each consisting of denaturation for 5 s at 98°C, annealing for 30 s at 60°C, and extension for 2 min at 68°C, in the presence of 3% (v/v) dimethyl sulfoxide using Pyrobest DNA Polymerase (Takara) and the plasmid DNA containing hCaMKP-N cDNA (AK289966, HuPEX clone FLJ76651) as the template. After gel purification, the amplified product was digested with *Eco*RV and *Sal*I and cloned into pCR4Blunt-TOPO (Invitrogen). The plasmid DNA was then sequenced with the ABI PRISM 3100 Genetic Analyzer (Applied Biosystems) to confirm the DNA sequence of the cloned insert. The plasmid was digested with *Eco*RV and *Sal*I, and the insert purified by gel purification was ligated into pEU-E01-MCS (CellFree Science) at the *Eco*RV and *Sal*I sites to generate pEU-E01-CaMKPN, which encodes the full-length hCaMKP-N with an N-terminal 6× His-tag. The pEU-E01-CaMKPN(1–559) vector, which encodes the C-terminal deletion mutant hCaMKP-N(1–559) with an N-terminal 6× His tag, was prepared using an inverse PCR mutagenesis kit (KOD-Plus-Mutagenesis Kit, TOYOBO) according to the manufacturer's instructions, with pEU-E01-CaMKPN as the template. The PCR was performed in a PC707 Thermal Cycler (ASTEC) for 10 cycles, each consisting of denaturation for 10 s at 98°C, annealing for 30 s at 60°C, and extension for 6 min at 68°C, in the presence of 4.8% (v/v) dimethyl sulfoxide with the sense primer (5′-TAG ATC CCA AAT CAA CGT GCT GGA AGA C-3′, underline shows the site of mutation) and the antisense primer (5′-TGG GCT CAG GCT AGT TCT ATC AGT G-3′). The PCR product was digested with *Dpn*I, and after gel purification, the amplified product was phosphorylated and self-ligated to generate pEU-E01-CaMKPN(1–559). The sequence of the mutated insert was confirmed by DNA sequencing.

2.3. The Cell-Free Expression of Recombinant hCaMKP-Ns and Its Purification. Cell-free expression of hCaMKP-N(WT) and hCaMKP-N(1–559) was carried out using a wheat-embryo cell-free protein expression system, the WEPRO 1240H Expression Kit (CellFree Sciences), according to the manufacturer's instruction, with either pEU-E01-CaMKPN or pEU-E01-CaMKPN(1–559). The *in vitro* translation reactions were conducted in a 96-well microtiter plate at 15°C for 18–20 hs. After the translation reaction, DNase-free RNase (24 μg/mL) and the cOmplete Mini EDTA-free protease inhibitor cocktail (Roche) (1 tablet/10 mL) were added to the translation reaction mixture, and the mixture was incubated for 30 min on ice. To 3 mL of the mixture, 0.96 mL of 50% (v/v) suspension of Ni^{2+}-Sepharose resin, which had been equilibrated and suspended in 20 mM Tris-HCl (pH 7.5) containing 0.2% (v/v) Tween 40, 10 mM imidazole, 300 mM NaCl, and 1 mM DTT, was added, and the mixture was then gently rocked at 4°C for 1 h. All of the following purification procedures were carried out at 4°C. The gel slurry was poured into an empty column (0.12 × 14 cm), and the flow-through fraction was allowed to drain. The column was washed with 5 mL of 20 mM Tris-HCl (pH 7.5) containing 0.05% (v/v) Tween 40, 20 mM imidazole, 1.5 M NaCl, and 1 mM DTT. For CaMKP-N(WT), the column was further washed with 2.5 mL of 20 mM Tris-HCl (pH 7.5) containing 0.05% (v/v) Tween 40, 100 mM imidazole, 300 mM NaCl, and 1 mM DTT, or for CaMKP-N(1–559), the column was further washed with 20 mM Tris-HCl (pH 7.5) containing 0.05% (v/v) Tween 40, 40 mM imidazole, 300 mM NaCl, and 1 mM DTT. The column was eluted with 2.5 mL of 20 mM Tris-HCl (pH 7.5) containing 0.05% (v/v) Tween 40, 250 mM imidazole, 300 mM NaCl, and 1 mM DTT, and the eluate was concentrated using a centrifugal filter unit (10,000 MWCO, Millipore). Glycerol was added to a final concentration of 30% (v/v). The purified enzymes were aliquoted and could be stored at −80°C for several months without any detectable loss in activity.

2.4. Protein Phosphatase Assays. Protein phosphatase assays using a phosphopeptide as a substrate were performed as previously described [13]. The phosphopeptides used in this study were derived from the amino acid sequence around the Thr286 autophosphorylation site on CaMKIIα (CaMKII(281–289) = pp2) or its analogs (pp4, pp6, pp10). The reaction was initiated by adding enzyme, and the reaction mixture was incubated at 30°C for 45 min. The amount of inorganic phosphate released in the mixture during the incubation was determined by malachite green assay [11]. The Michaelis-Menten kinetic parameters were determined from a direct fit to the Michaelis-Menten equation using a nonlinear regression program (DeltaGraph, version 6.0,

Red Rock Software) as previously described [11]. The tested compounds were added to the reaction systems mentioned above at the indicated concentrations.

The protein phosphatase assay using autophosphorylated CaMKII as a phosphoprotein substrate was performed as described [13] with the following modifications. The PSD fraction (905 μg/mL) was incubated at 5°C for 10 min in the reaction mixture (100 μL) containing 40 mM Hepes-NaOH (pH 8.0), 5 mM $Mg(CH_3COO)_2$, 0.1 mM EGTA, 1 μM calmodulin, 0.8 mM $CaCl_2$, 0.01% Tween 20, and 50 μM nonradioactive ATP to autophosphorylate the CaMKII found in the PSD fraction. After the reaction, the mixture was immediately diluted with 1 mL of ice-cold wash buffer consisting of 50 mM Tris-HCl (pH 7.5), 0.2 M NaCl, 0.05% Tween 40, 0.1 μM calyculin A, and 0.1 mM DTT, and then it was centrifuged for 10 min at 4°C in a microcentrifuge at maximum speed. The supernatant was removed, and the precipitate was resuspended with the ice-cold wash buffer and centrifuged again as described previously. The washing procedure was repeated five more times. The precipitate obtained was resuspended in 100 μL of the washing buffer and stored at −80°C until it was used. The phosphatase reaction was carried out in a reaction mixture containing 50 mM Tris-HCl (pH 7.5), 2 mM $MnCl_2$, 0.1 mM EGTA, and 0.01% Tween 20. Western blotting analysis using anti-active CaMKII (anti-PCaMKII, 1 : 1000 dilution) was performed to estimate the extent of autophosphorylation at the Thr286 site on CaMKII. After the detection of autophosphorylated CaMKII, the blot was treated with Blot Restorte Membrane Rejuvenation Kit (Millipore) according to the manufacturer's instructions, so that it could be reprobed. To confirm the amount of total CaMKII on the blot, the rejuvenated blot was reprobed with a monoclonal anti-CaMKIIα (CBα-2, 1 : 500 dilution).

2.5. Binding of hCaMKP-N(1–559) to PSD. hCaMKP-N(1–559) (1 μg) was incubated with the PSD fraction (1 μg) in 50 mM Tris-HCl (pH 7.5) (10 μL) on ice for 1 h and then centrifuged for 5 min at 4°C in a microcentrifuge at maximum speed. The pellet fraction was suspended with ice-cold 50 mM Tris-HCl (pH 8.1) containing 0.85% NaCl (1 mL), and the suspension was centrifuged as described previously. The washing procedure was repeated, and the pellet fraction was resuspended in a minimum volume of 50 mM Tris-HCl (pH 8.1) containing 0.85% NaCl. An equal volume of 2× SDS-sample buffer was added to the suspension to prepare the samples for western blotting analysis.

2.6. Western Blotting Analysis. The protein samples were separated by gel electrophoresis and transferred onto an Immobilon-P polyvinylidene difluoride membrane (Millipore) as previously described [14]. After blocking, the membrane was incubated overnight at 4°C with primary antibodies and then incubated with the biotinylated rabbit anti-mouse IgG (1 : 2000 dilution) or anti-rabbit Ig biotinylated species-specific antibody (1 : 2000 dilution) for 2 h at room temperature. This step was followed by incubation with a streptavidin-horseradish peroxidase conjugate (1 : 500 dilution) for 40 min at room temperature. The western blots were visualized by an enhanced chemiluminescence detection procedure using LAS-1000 (GE Healthcare) image analyzers.

2.7. Other Analytical Methods. SDS-PAGE was carried out according to the Laemmli method [15]. Protein concentrations were determined using an advanced protein assay reagent (cytoskeleton) with bovine serum albumin as a standard. The concentrations of the pp2 and pp4 peptides were determined by measuring the Pi released after alkali hydrolysis as previously described [11]. The concentration of the pp6 peptide was determined by measuring the Pi released after acid hydrolysis as previously described [11]. The concentration of the pp10 peptide was determined spectrophotometrically using the absorption coefficient for tyrosine ($\varepsilon_{278} = 1.16 \times 10^3\ M^{-1}\ cm^{-1}$).

3. Results

3.1. Preparation of hCaMKP-N and hCaMKP-N(1–559) Using a Wheat-Embryo Cell-Free Protein Expression System. It has been reported that CaMKP-N undergoes proteolytic processing in the rat brain to generate a 90 kDa fragment in which the C-terminal region is truncated [10]. In an attempt to evaluate the physiological significance of the C-terminal truncation of hCaMKP-N, we prepared full-length and truncated hCaMKP-N to compare their enzymatic properties. Kitani et al. [10] reported that rat CaMKP-N is truncated at or near Pro554. Since the amino acid sequence identity between rat and human CaMKP-N is very high (88%) [16], we constructed expression plasmids for the full-length hCaMKP-N (hCaMKP-N(WT)) and for the truncated hCaMKP-N fragment, in which the C-terminal side of the corresponding Pro residue (Pro559) was deleted, (hCaMKP-N(1–559)), and both contain an added 6× His-tag at their N-terminus (Figure 1(b)). Using the expression plasmids as templates, we synthesized the full-length hCaMKP-N and hCaMKP-N(1–559) proteins with a wheat-embryo cell-free protein expression system and purified these enzymes by Ni^{2+}-Sepharose affinity chromatography as described in Section 2. The purified hCaMKP-N(WT) and hCaMKP-N(1–559) showed apparent molecular masses of approximately 120 kDa and 90 kDa on SDS-PAGE, respectively (Figure 2(a)), which are in good agreement with the previous report [5]. Both enzymes were detected by the anti-CaMKP-N antibody that was raised against a synthetic peptide corresponding to the 474–488 region of zCaMKP-N (Figure 2(b)). Because this region shares fairly high homology with the region that is N-terminal side to Pro559 on hCaMKP-N (Figure 1(b)) [8], it was confirmed that the purified phosphatases retained the N-terminal side of Pro559. It should be noted that the hCaMKP-N(WT) preparation was essentially free from the 90 kDa proteolytic fragment usually seen in the preparations purified from the baculovirus-transfected Sf9 cells [5].

3.2. Activation of hCaMKP-N by C-Terminal Truncation. Using the protein preparations described previously, the

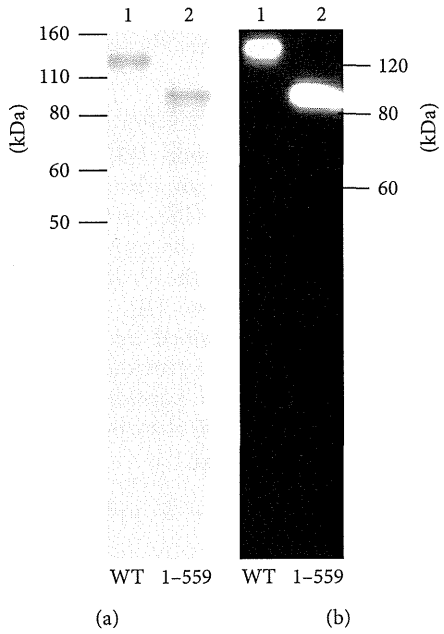

FIGURE 2: hCaMKP-N and its truncation mutant prepared by a wheat-embryo cell-free protein expression system. (a) hCaMKP-N(WT) (lane 1, 2.5 μg) and hCaMKP-N(1–559) (lane 2, 2.5 μg), which had been prepared and purified as described in Section 2, were subjected to SDS-PAGE on a 10% polyacrylamide gel. The gel was stained with Coomassie Brilliant Blue (CBB) using Quick CBB. (b) hCaMKP-N(WT) (lane 1) and hCaMKP-N(1–559) (lane 2) were subjected to SDS-PAGE on a 10% polyacrylamide gel and analyzed by western blotting analysis using an anti-CaMKP-N antibody (1 : 250 dilution) as the primary antibody.

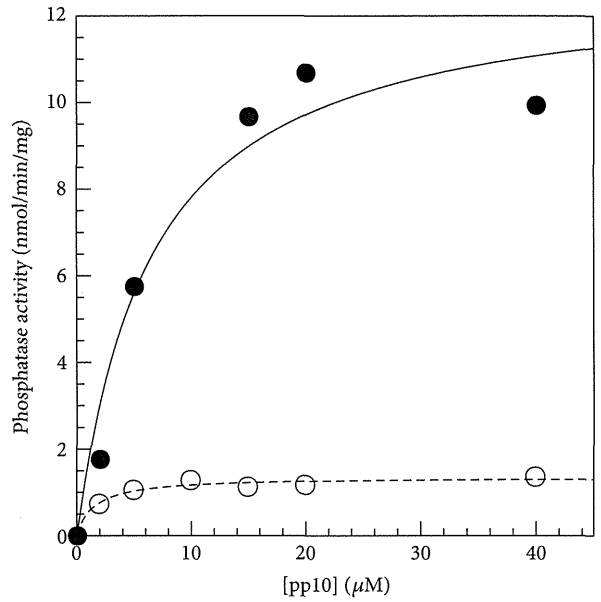

FIGURE 3: Dephosphorylation of a phosphopeptide substrate pp10 by hCaMKP-N(WT) and hCaMKP-N(1–559). The indicated concentrations of pp10 were dephosphorylated by hCaMKP-N(WT) (open circles) and by hCaMKP-N(1–559) (closed circles) at 30°C as described in Section 2. The amount of inorganic phosphate released in the reaction mixture during the reaction was determined as described. The indicated curves were obtained by direct fits of the data to Michaelis-Menten equation. The data shown are those in a representative experiment of at least three independent determinations with similar results.

kinetic properties of hCaMKP-N(WT) and hCaMKP-N(1–559) were evaluated and compared. The phosphatase activities were assessed under the standard assay conditions for CaMKP and CaMKP-N [5, 11], where they were assayed in the presence of 2 mM Mn^{2+} using the pp10 phosphopeptide as a substrate (Figure 3). hCaMKP-N(1–559) showed much higher activity than hCaMKP-N(WT). We performed a kinetic analysis of hCaMKP-N(WT) and hCaMKP-N(1–559) with varying concentrations of the pp10 substrate. They displayed typical Michaelis-Menten kinetics, and the K_m value for pp10 and the V_{max} value were determined (Figure 3, Table 1). These parameters strongly suggested that the truncation of the C-terminal region of hCaMKP-N results in a marked increase in the V_{max} for the phosphatase activity.

3.3. Some Enzymatic Properties of hCaMKP-N(1–559). Since the C-terminally truncated form has been reported to be the most abundant species of CaMKP-N in the rat brain [10], the enzymatic properties of hCaMKP-N(1–559) were further examined using pp10 as the substrate. As shown in Figure 4(a), the truncated fragment showed a strong Mn^{2+}-dependent phosphatase activity and a weak Mg^{2+}-dependent phosphatase activity but no Ca^{2+}-dependent activity. We also examined the effect of varying concentrations of Mn^{2+} and Mg^{2+} on the phosphatase activity (Figure 4(b)). Only a

TABLE 1: Comparison of the phosphatase activities of hCaMKP-N(WT) and hCaMKP-N(1–559). hCaMKP-N(WT) and hCaMKP-N(1–559) were assayed using varying concentrations of the pp10 substrate as described in Section 2. Michaelis-Menten kinetic parameters were determined from a direct fit to the Michaelis-Menten equation. The data represent the average of three independent experiments ± S.D.

	K_m (μM)	V_{max} (nmol/min/mg)
hCaMKP-N(WT)	2.0 ± 0.9	1.4 ± 0.1
hCaMKP-N(1–559)	5.4 ± 0.1	16.3 ± 3.6

submillimolar concentration of Mn^{2+} was required for the full activity of hCaMKP-N(1–559), whereas more than 10 mM Mg^{2+} was required for the same level of activity. A kinetic analysis revealed that the half-maximal activations for Mn^{2+} and Mg^{2+} are 0. 22 ± 0.04 mM and 6.4 ± 1.6 mM, respectively. It should be noted that almost the same level of full activity was observed at their saturating levels, regardless of whether Mn^{2+} or Mg^{2+} was used as a cofactor.

It has been reported that PPM family phosphatases, including PP2C and CaMKP, strongly prefer phospho-Thr over phospho-Ser as the residue to be dephosphorylated [11, 17]. Therefore, we examined the phosphoamino acid residue preference of hCaMKP-N(1–559). For this purpose,

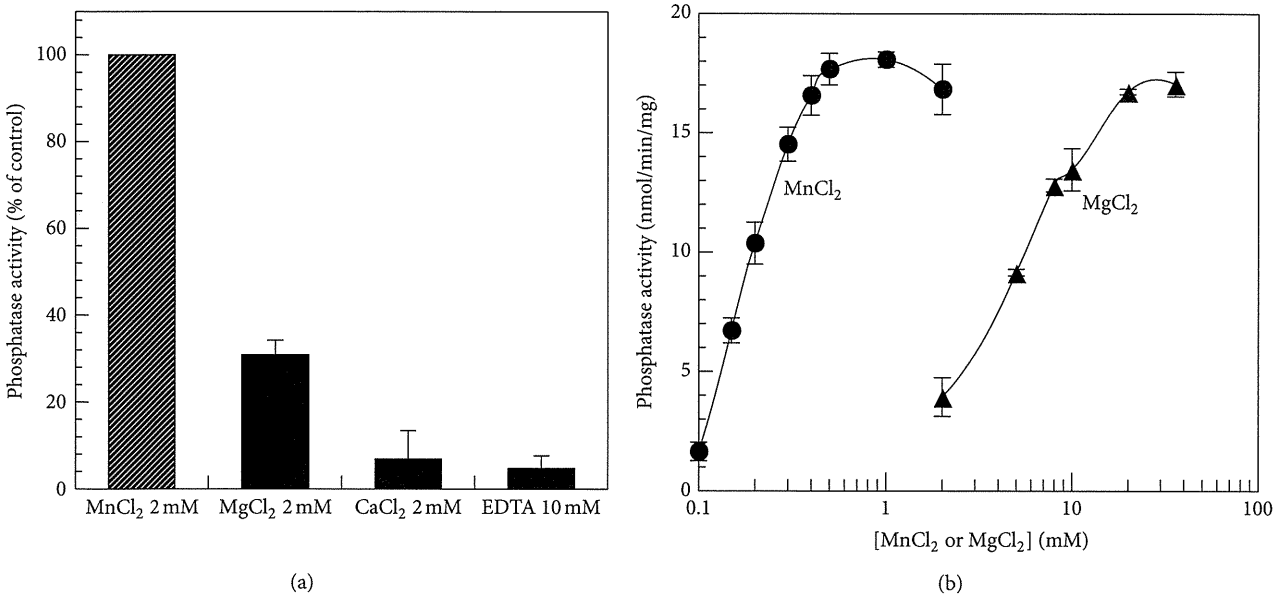

FIGURE 4: The divalent cation requirement for the phosphatase activity of hCaMKP-N(1–559). (a) hCaMKP-N(1–559) was assayed using pp10 as the substrate in the presence of the indicated divalent cations or EDTA instead of 2 mM $MnCl_2$ as described in Section 2. The results are expressed as the percentage of the activity determined with 2 mM $MnCl_2$. The data represent the average of three independent experiments ± S.D. (b) hCaMKP-N(1–559) was assayed using pp10 as the substrate in the presence of varying concentrations of $MnCl_2$ (circles) or $MgCl_2$ (triangles) instead of 2 mM $MnCl_2$.

a synthetic phospho-CaMKII(281–289) peptide (named pp2) and its analogs, in which phospho-Thr was replaced with phospho-Ser (named pp4) or with phospho-Tyr (named pp6), were used as substrates for hCaMKP-N(1–559). The truncated hCaMKP-N efficiently dephosphorylated the parent phospho-Thr peptide pp2, but it barely dephosphorylated the phospho-Ser peptide (pp4) and the phospho-Tyr peptide (pp6), indicating strong preference for phospho-Thr residues as was observed for other PPM family phosphatases (Figure 5).

The effects of some protein phosphatase inhibitors on hCaMKP-N(1–559) were also examined and are shown in Figure 6. Okadaic acid (1 μM) and calyculin A (1 μM), potent PP1 and PP2A inhibitors, had no effect on the phosphatase activity. This is because hCaMKP-N is classified as PPM family phosphatases of which structures are quite different from those of PPP family phosphatases such as PP1 and PP2A. In contrast, NaF (100 mM) and EDTA (10 mM) severely inhibited the phosphatase. It is interesting that ANDS, a CaMKP-specific inhibitor [18], did not inhibit the phosphatase activity of hCaMKP-N(1–559) even at 30 μM, a concentration at which the rat CaMKP was strongly inhibited.

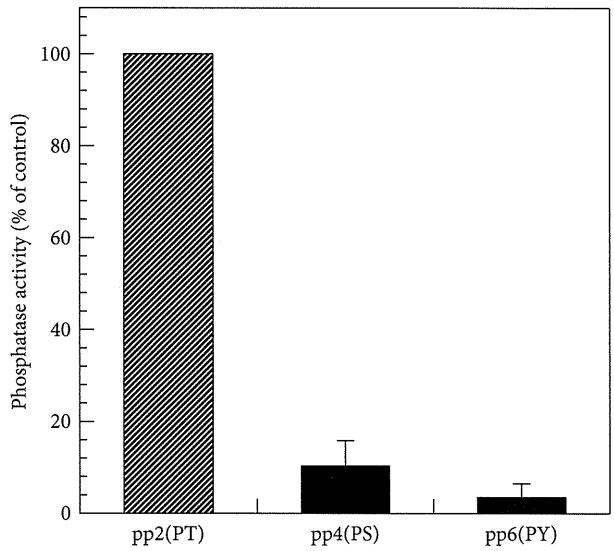

FIGURE 5: The residue preference at the dephosphorylation site. hCaMKP-N(1–559) was assayed using the indicated phosphopeptides (20 μM) as substrates under the standard assay conditions as described in Section 2. The results are expressed as a percentage of the activity determined using pp2 as the substrate. The data represent the average of three independent experiments ± S.D.

3.4. Dephosphorylation of the Autophosphorylated CaMKII in PSD by hCaMKP-N(1–559). CaMKII, one of the candidates for the physiological substrate of hCaMKP-N(1–559), is known to exist abundantly in PSD. Therefore, we examined interaction of hCaMKP-N(1–559) and the rat brain PSD as described in Section 2. The endogenous rat CaMKP-N fragment was not detected in the isolated PSD fraction prepared from the rat brain (Figure 7(a), lane 1). Sequence homology between the rat and human CaMKP-N and the sequence homology between the rat and human CaMKIIα are very high (88% and 99% identity, resp.). After the PSD fraction was incubated with hCaMKP-N(1–559) on ice for 1 h, a significant amount of the CaMKP-N fragment was detected in the PSD fraction (Figure 7(a), lane 2).

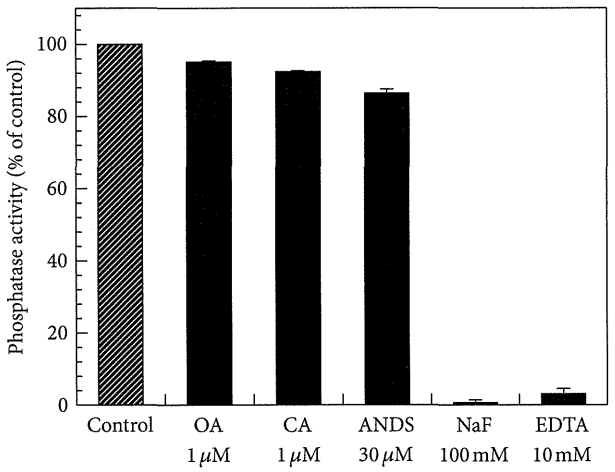

FIGURE 6: The effects of various inhibitors on the phosphatase activity of hCaMKP-N(1–559). hCaMKP-N(1–559) was assayed using pp10 as the substrate in the presence of the indicated compounds. The results are expressed as a percentage of the activity determined with no compound added (control). The abbreviations used in the figure are as follows: OA: okadaic acid; CA: calyculin A; ANDS: 1-amino-8-naphthol-2,4-disulfonic acid. The data represent the average of three independent experiments ± S.D.

Since the PSD-associated CaMKP-N fragment may play a physiological role, the phosphatase activity of hCaMKP-N(1–559) on the autophosphorylated CaMKII was examined. The endogenous CaMKII in the rat PSD fraction was autophosphorylated in the presence of Ca^{2+}/calmodulin and was used as a substrate for hCaMKP-N(1–559). Under the autophosphorylation conditions used, no significant band shift for the CaMKIIα subunit was observed by SDS-PAGE. As shown in Figure 7(b), the autophosphorylated CaMKII was dephosphorylated by hCaMKP-N(1–559) (lane 2). Therefore, hCaMKP-N(1–559) can bind to PSD to dephosphorylate the autophosphorylated CaMKII.

3.5. The Reversible Regulation of hCaMKP-N(1–559) by Oxidation/Reduction. We have reported that incubation of human CaMKP with H_2O_2 leads to the formation of a disulfide bond, which results in inactivation of the enzyme [19]. As shown in Figure 8(a), H_2O_2 also inactivated hCaMKP-N(1–559) in a dose-dependent manner. When the inactivated hCaMKP-N(1–559) was further incubated on ice for 30 min with the reducing agent DTT, the phosphatase activity was restored to almost original levels (Figure 8(b)). This indicates that the inactivation of hCaMKP-N(1–559) by H_2O_2 is a reversible process and that hCaMKP-N(1–559) is reversibly regulated by oxidation/reduction.

4. Discussion

Based on the subcellular localization of transiently expressed hCaMKP-N in COS cells [5], it had been assumed that mammalian CaMKP-N is localized only in the nucleus. However, Kitani et al. [10] showed that in the rat brain, CaMKP-N undergoes proteolytic processing to form a 90 kDa fragment that is localized mainly in the cytosol. Similar proteolytic fragment of CaMKP-N was also found in human frontal cortex [20]. Therefore, the truncated form of hCaMKP-N may have important functions in cells.

In this study, we used a wheat-embryo cell-free protein expression system for preparation of hCaMKP-N and its fragment to minimize proteolysis during the expression and purification of hCaMKP-N. Using this system in conjunction with conventional Ni^{2+}-NTA agarose chromatography, we were able to individually prepare the full-length hCaMKP-N, hCaMKP-N(WT), and its proteolytic fragment, hCaMKP-N(1–559), for the first time without mutual contamination. Typically, approximately 15 μg of purified hCaMKP-N or its fragment could be obtained from 1 well of a translation reaction mixture (21 μL of the wheat-embryo translation mixture and 206 μL of the substrate solution) in a 96-well microtiter plate (data not shown). The wheat-embryo cell-free protein expression system has been proven useful for the preparation of the proteins that are readily degraded by cellular proteases. Because the protease activities detected in the cell-free system are very low [21, 22], this method may be applicable to other protease-sensitive proteins that are difficult to prepare using conventional cell-based expression systems such as Sf9 cells.

Using these preparations, we could rigorously compare the catalytic properties of hCaMKP-N(1–559) and hCaMKP-N(WT). Both hCaMKP-N species have phosphatase activities in the presence of Mn^{2+} toward the pp10 phosphopeptide substrate, which was based on the amino acid sequence around the critical Thr286 autophosphorylation site on CaMKII. This result indicates that the proteolytic fragment is not a degraded and inactive species, but instead, it has phosphatase activity. Although the K_m value for the fragment was somewhat higher than the K_m value for the hCaMKP-N(WT), the V_{max} value for the fragment was more than ten times higher than that for the WT. Therefore, we suggest that the truncation of C-terminal region 560–757 of hCaMKP-N is a post-translational regulatory mechanism to generate a highly active species.

The mechanism of activation by truncation remains unclear. The truncated C-terminal region might act as an autoinhibitory domain, as is the case for calcineurin [23]. Alternatively, processing of the region might cause a conformational change in its catalytic center that leads to catalytic activation. It has been reported that some protein phosphatases in the PPP family are activated by proteolysis [24, 25]. We have also reported that zCaMKP-N is activated by proteolytic processing of the C-terminal domain [9]. Therefore, activation by C-terminal truncation appears to be a common feature for CaMKP-N, despite the fact that hCaMKP-N and zCaMKP-N have fairly different molecular sizes and primary structures. Because it has been reported that rat CaMKP-N(1–554), a fragment corresponding to hCaMKP-N(1–559), is localized in the cytosol of transfected COS cells [10], the truncation of the C-terminal domain is likely to regulate catalytic activity as well as the intracellular localization of hCaMKP-N. Since inhibition of the proteolytic processing of zCaMKP-N in Neuro2a cells by proteasome

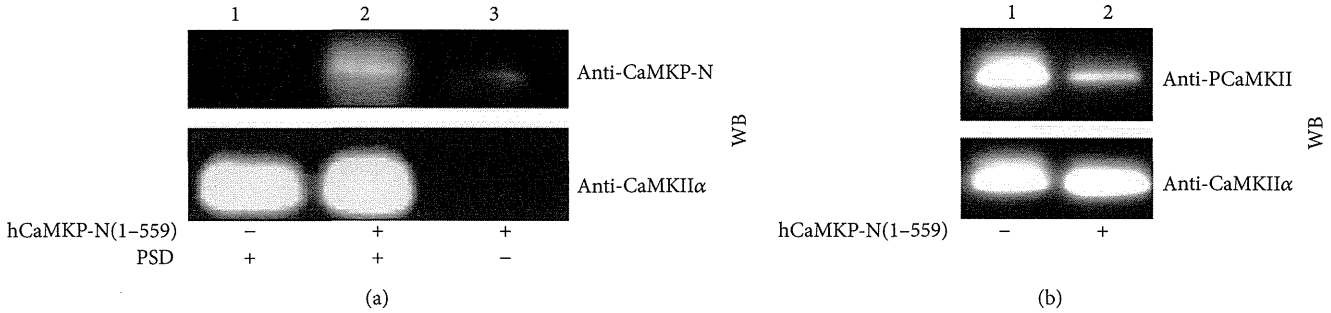

FIGURE 7: The binding of hCaMKP-N(1–559) to PSD and the dephosphorylation of the autophosphorylated CaMKII. (a) hCaMKP-N(1–559) (1 μg) was incubated on ice for 1 h with (lane 2) or without (lane 3) the PSD fraction (1 μg) as described in Section 2. After incubation, the mixture was centrifuged, and the pellet fraction was washed twice with 50 mM Tris-HCl (pH 7.5) containing 0.85% NaCl, followed by western blotting analysis using anti-CaMKP-N antibody (upper panel). Recovery of the PSD fraction was confirmed by probing the same blot using anti-CaMKIIα antibody (lower panel). To check the endogenous CaMKP-N levels, the PSD fraction was also incubated in the absence of hCaMKP-N(1–559) as a control (lane 1). (b) The PSD fraction (29 μg/mL), in which CaMKII had been autophosphorylated as described, was incubated at 30°C with (lane 2) or without (lane 1) hCaMKP-N(1–559). After incubation for 30 min, the phosphatase reaction was terminated by adding excess EDTA (20 mM), and aliquots were analyzed by western blotting to examine the extent of phosphorylation at Thr286 on CaMKII (upper panel, anti-PCaMKII) and the total amount of CaMKIIα on the blot (lower panel, anti-CaMKIIα). The data presented are representative of at least three independent experiments with similar results.

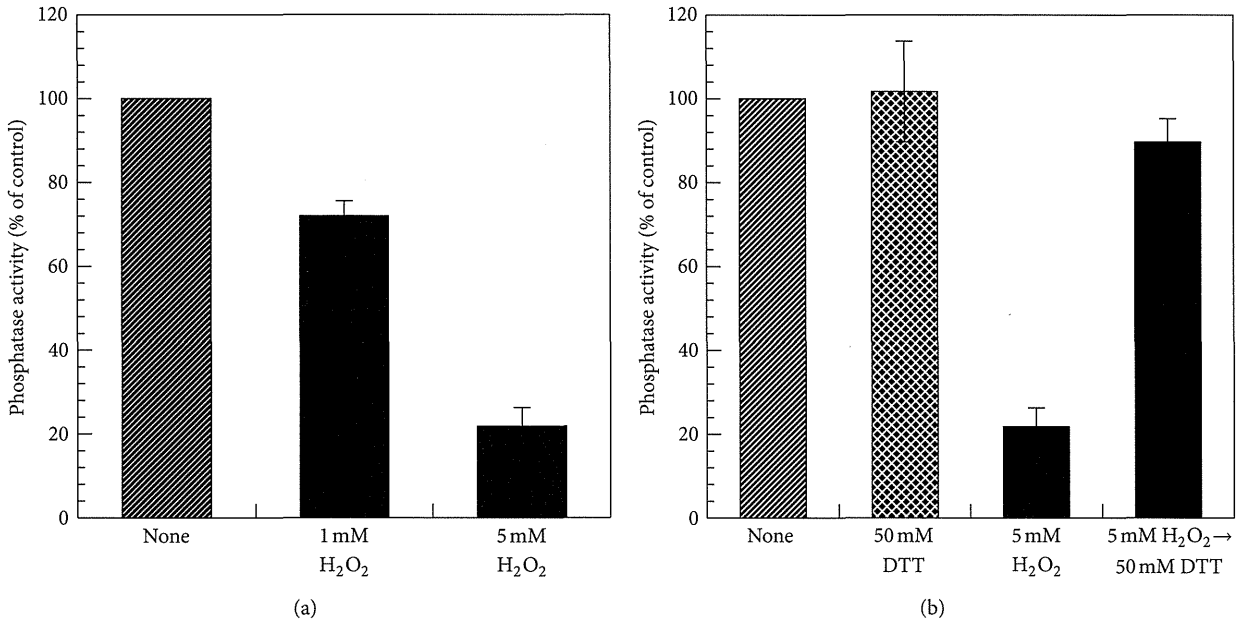

FIGURE 8: The reversible inactivation of hCaMKP-N(1–559) by H_2O_2. (a) hCaMKP-N(1–559) (245 μg/mL) was incubated on ice for 30 min in 25 mM Tris-HCl (pH 7.5) with or without the indicated concentrations of H_2O_2, and then the phosphatase activities were determined using pp1α as the substrate. (b) hCaMKP-N(1–559) (245 μg/mL) was incubated on ice for 30 min in 25 mM Tris-HCl (pH 7.5) with 5 mM H_2O_2, and then DTT (50 mM) was added for incubation on ice for an additional 30 min. Thereafter, the phosphatase activity was determined using pp1α as the substrate. As a comparison, the phosphatase activity without DTT treatment is also presented (5 mM H_2O_2). The DTT treatment itself had no significant effects on the activity of hCaMKP-N(1–559) in the control (50 mM DTT). The results are expressed as a percentage of the control activity (none), which was determined after incubation without any compounds (H_2O_2 or DTT) added. The data represent the average of three independent experiments ± S.D.

inhibitors significantly changed substrate targeting in the cells [9], activation and translocation of the mammalian CaMKP-N may also affect the intracellular substrate targeting.

The activated CaMKP-N fragment generated by the proteolytic processing is reported to be the major species of CaMKP-N in the rat brain [10]. Here, we show a molecular characterization of the 90 kDa active fragment in human, hCaMKP-N(1–559). It exhibited okadaic acid/calyculin A-insensitive and Mn^{2+} or Mg^{2+}-dependent phosphatase activity and demonstrated a striking preference for a phosphothreonyl peptide over a phosphoseryl or a phosphotyrosyl

peptide. These enzymatic properties are similar to those of CaMKP [11]. However, the metal dependence of hCaMKP(1–559) was somewhat different from that of CaMKP. Although the half-maximal activation for Mn^{2+} is comparable to that of rat CaMKP (~0.2 mM), activation by Mg^{2+} is more prominent in hCaMKP(1–559) than it is in CaMKP [26]. Furthermore, hCaMKP-N(1–559) showed Mn^{2+}-dependent activity and comparable Mg^{2+}-dependent activity at its saturating levels. NaF is known to inhibit various protein phosphatases. Fluoride is reported to directly bind to the metal ions in the active center of bovine purple acid phosphatase [27]. Since Ser/Thr protein phosphatases are known to be metalloenzymes that employ dinuclear metal center similar to purple acid phosphatases [28], it is most likely that fluoride also binds to the metal center to inhibit its phosphatase activity. Interestingly, ANDS, a potent inhibitor for CaMKP [18], did not inhibit the phosphatase activity of hCaMKP-N(1–559). This suggests that the three-dimensional structure of the active site of hCaMKP-N is considerably different from that of rat CaMKP even though their primary structures of their putative catalytic regions are highly homologous.

hCaMKP-N(1–559) could bind to PSD to dephosphorylate the CaMKII associated with it. Based on electron microscope results, the corresponding CaMKP-N fragment is suggested to be concentrated in PSD together with CaMKII in rat brain [10]; however, the endogenous rat CaMKP-N fragment was not detected in the isolated PSD fraction. Therefore, it is likely that the CaMKP-N fragment is not a component of PSD, but its binding to PSD is dynamically regulated in neuronal cells. This fragment might be involved in regulation of CaMKII activity in PSD, where synaptic transmission is tightly controlled. The CaMKP-N activated by proteolysis might be a critical regulator for synaptic transmission through controlling the phosphorylation state of the CaMKII in PSD.

Another notable finding in this study is that hCaMKP-N(1–559) is inactivated by H_2O_2 treatment, and reactivated by incubation with DTT. Recently, we reported that human CaMKP is reversibly regulated by oxidation/reduction at Cys359 [19]. This Cys residue is adjacent to an Asp residue that is essential for metal binding at the active site, and the Cys-Asp sequence is conserved in the catalytic sites of many PPM family enzymes including hCaMKP-N. Therefore, the observed inactivation of hCaMKP-N(1–559) might be due to reversible oxidation at Cys436 of hCaMKP-N. The reversible regulation of the phosphatase activity of hCaMKP-N(1–559) by oxidation/reduction may be an important mechanism for regulating the phosphorylation levels of CaMKII in neuronal cells, especially in PSD, in response to oxidative stress.

In summary, we showed for the first time that hCaMKP-N is activated through truncation of the C-terminal domain. The active truncated fragment could bind to PSD to dephosphorylate CaMKII, and its enzymatic properties were similar to those of CaMKP except for its Mg^{2+}-dependence and sensitivity to ANDS. Very recently, genome-wide association studies suggested that single nucleotide polymorphisms found in the loci for CaMKP-N (PPM1E) and for CaMKP (PPM1F) are associated with testicular germ cell tumor [29] and with both schizophrenia and bipolar disorders [30], respectively. Since hCaMKP-N(1–559) is supposedly localized in the cytosol where CaMKP is found, the next important question concerns what are the roles that CaMKP and the active CaMKP-N fragment share in the cytosol. Further work is needed to address this question.

Abbreviations

ANDS: 1-Amino-8-naphthol-2,4-disulfonic acid
CaMKII: Ca^{2+}/calmodulin-dependent protein kinase II
CaMKP: Ca^{2+}/calmodulin-dependent protein kinase phosphatase
hCaMKP-N: Human Ca^{2+}/calmodulin-dependent protein kinase phosphatase-N
PSD: Postsynaptic density
zCaMKP-N: Zebrafish Ca^{2+}/calmodulin-dependent protein kinase phosphatase-N.

Conflict of Interests

The authors reveal that there is no conflict of interests in this paper.

Acknowledgments

This work was supported, in part, by Grants-in-Aid for Scientific Research (21590334) from the Ministry of Education, Science, Sports, and Culture of Japan and by a grant from the Japan Foundation for Applied Enzymology.

References

[1] A. Ishida, I. Kameshita, and H. Fujisawa, "A novel protein phosphatase that dephosphorylates and regulates Ca^{2+}/calmodulin-dependent protein kinase II," *Journal of Biological Chemistry*, vol. 273, no. 4, pp. 1904–1910, 1998.

[2] A. Ishida, S. Okuno, T. Kitani, I. Kameshita, and H. Fujisawa, "Regulation of multifunctional Ca^{2+}/calmodulin-dependent protein kinases by Ca^{2+}/calmodulin-dependent protein kinase phosphatase," *Biochemical and Biophysical Research Communications*, vol. 253, no. 1, pp. 159–163, 1998.

[3] T. Kitani, A. Ishida, S. Okuno, M. Takeuchi, I. Kameshita, and H. Fujisawa, "Molecular cloning of Ca^{2+}/calmodulin-dependent protein kinase phosphatase," *Journal of Biochemistry*, vol. 125, no. 6, pp. 1022–1028, 1999.

[4] A. Ishida, N. Sueyoshi, Y. Shigeri, and I. Kameshita, "Negative regulation of multifunctional Ca^{2+}/calmodulin-dependent protein kinases: physiological and pharmacological significance of protein phosphatases," *British Journal of Pharmacology*, vol. 154, no. 4, pp. 729–740, 2008.

[5] M. Takeuchi, A. Ishida, I. Kameshita, T. Kitani, S. Okuno, and H. Fujisawa, "Identification and characterization of CaMKP-N, nuclear calmodulin-dependent protein kinase phosphatase," *Journal of Biochemistry*, vol. 130, no. 6, pp. 833–840, 2001.

[6] C. Koh, E. Tan, E. Manser, and L. Lim, "The p21-activated kinase PAK is negatively regulated by POPX1 and POPX2, a pair of serine/threonine phosphatases of the PP2C family," *Current Biology*, vol. 12, no. 4, pp. 317–321, 2002.

[7] M. Voss, J. Paterson, I. R. Kelsall et al., "Ppm1E is an in cellulo AMP-activated protein kinase phosphatase," *Cellular Signalling*, vol. 23, no. 1, pp. 114–124, 2011.

[8] T. Nimura, N. Sueyoshi, A. Ishida et al., "Knockdown of nuclear Ca^{2+}/calmodulin-dependent protein kinase phosphatase causes developmental abnormalities in zebrafish," *Archives of Biochemistry and Biophysics*, vol. 457, no. 2, pp. 205–216, 2007.

[9] N. Sueyoshi, T. Nimura, T. Onouchi et al., "Functional processing of nuclear Ca^{2+}/calmodulin-dependent protein kinase phosphatase (CaMKP-N): evidence for a critical role of proteolytic processing in the regulation of its catalytic activity, subcellular localization and substrate targeting in vivo," *Archives of Biochemistry and Biophysics*, vol. 517, no. 1, pp. 43–52, 2012.

[10] T. Kitani, S. Okuno, Y. Nakamura, H. Tokuno, M. Takeuchi, and H. Fujisawa, "Post-translational excision of the carboxyl-terminal segment of CaM kinase phosphatase N and its cytosolic occurrence in the brain," *Journal of Neurochemistry*, vol. 96, no. 2, pp. 374–384, 2006.

[11] A. Ishida, Y. Shigeri, Y. Tatsu et al., "Substrate specificity of Ca^{2+}/calmodulin-dependent protein kinase phosphatase: kinetic studies using synthetic phosphopeptides as model substrates," *Journal of Biochemistry*, vol. 129, no. 5, pp. 745–753, 2001.

[12] N. Sahyoun, H. LeVine III, and D. Bronson, "Cytoskeletal calmodulin-dependent protein kinase. Characterization, solubilization, and purification from rat brain," *Journal of Biological Chemistry*, vol. 260, no. 2, pp. 1230–1237, 1985.

[13] T. Onouchi, N. Sueyoshi, A. Ishida, and I. Kameshita, "Phosphorylation and activation of nuclear Ca^{2+}/calmodulin-dependent protein kinase phosphatase (CaMKP-N/PPM1E) by Ca^{2+}/calmodulin-dependent protein kinase I, (CaMKI)," *Biochemical and Biophysical Research Communication*, vol. 422, no. 4, pp. 703–709, 2012.

[14] E. Harlow and D. Lane D, *Antibodies: A Laboratory Manual*, Cold Spring Harbor Laboratory Press, Cold Spring Harbor, NY, USA, 1988.

[15] U. K. Laemmli, "Cleavage of structural proteins during the assembly of the head of bacteriophage T4," *Nature*, vol. 227, no. 5259, pp. 680–685, 1970.

[16] T. Kitani, S. Okuno, M. Takeuchi, and H. Fujisawa, "Subcellular distributions of rat CaM kinase phosphatase N and other members of the CaM kinase regulatory system," *Journal of Neurochemistry*, vol. 86, no. 1, pp. 77–85, 2003.

[17] A. Donella Deana, C. H. Mac Gowan, P. Cohen, F. Marchiori, H. E. Meyer, and L. A. Pinna, "An investigation of the substrate specificity of protein phosphatase 2C using synthetic peptide substrates; Comparison with protein phosphatase 2A," *Biochimica et Biophysica Acta*, vol. 1051, no. 2, pp. 199–202, 1990.

[18] N. Sueyoshi, T. Takao, T. Nimura et al., "Inhibitors of the Ca^{2+}/calmodulin-dependent protein kinase phosphatase family (CaMKP and CaMKP-N)," *Biochemical and Biophysical Research Communications*, vol. 363, no. 3, pp. 715–721, 2007.

[19] H. Baba, N. Sueyoshi, Y. Shigeri, A. Ishida, and I. Kameshita, "Regulation of Ca^{2+}/calmodulin-dependent protein kinase phosphatase (CaMKP) by oxidation /reduction at Cys-359," *Archives of Biochemistry and Biophysics*, vol. 526, no. 1, pp. 9–15, 2012.

[20] A. L. Jessen, *Characterization of the protein phosphatase 1E (PPM1E): localization and truncation in brain tissue and effects on neuronal morphology in primary neuronal culture [Ph.D. thesis]*, Georg August University of Göttingen, Faculty of Biology, Göttingen, Germany, 2010, *Dissertation in partial fulfillment of the requirements for the degree "Doctor rerum naturalium"*, http://ediss.uni-goettingen.de/handle/11858/00-1735-0000-0006-ADD4-0.

[21] T. Sawasaki, Y. Hasegawa, R. Morishita, M. Seki, K. Shinozaki, and Y. Endo, "Genome-scale, biochemical annotation method based on the wheat germ cell-free protein synthesis system," *Phytochemistry*, vol. 65, no. 11, pp. 1549–1555, 2004.

[22] H. Takahashi, A. Nozawa, M. Seki, K. Shinozaki, Y. Endo, and T. Sawasaki, "A simple and high-sensitivity method for analysis of ubiquitination and polyubiquitination based on wheat cell-free protein synthesis," *BMC Plant Biology*, vol. 9, Article ID 39, 2009.

[23] Y. Hashimoto, B. A. Perrino, and T. R. Soderling, "Identification of an autoinhibitory domain in calcineurin," *Journal of Biological Chemistry*, vol. 265, no. 4, pp. 1924–1927, 1990.

[24] C. Sinclair, C. Borchers, C. Parker, K. Tomer, H. Charbonneau, and S. Rossie, "The tetratricopeptide repeat domain and a C-terminal region control the activity of Ser/Thr protein phosphatase 5," *Journal of Biological Chemistry*, vol. 274, no. 33, pp. 23666–23672, 1999.

[25] H. Y. Wu, K. Tomizawa, Y. Oda et al., "Critical role of calpain-mediated cleavage of calcineurin in excitotoxic neurodegeneration," *Journal of Biological Chemistry*, vol. 279, no. 6, pp. 4929–4940, 2004.

[26] N. Sueyoshi, T. Nimura, A. Ishida et al., "Ca^{2+}/calmodulin-dependent protein kinase phosphatase (CaMKP) is indispensable for normal embryogenesis in zebrafish, Danio rerio," *Archives of Biochemistry and Biophysics*, vol. 488, no. 1, pp. 48–59, 2009.

[27] M. W. Pinkse, M. Merkx, and B. A. Averill, "Fluoride inhibition of bovine spleen purple acid phosphatase: characterization of a ternary enzyme-phosphate-fluoride complex as a model for the active enzyme-substrate-hydroxide complex," *Biochemistry*, vol. 38, no. 31, pp. 9926–9936, 1999.

[28] D. Barford, A. K. Das, and M. Egloff, "The structure and mechanism of protein phosphatases: insights into catalysis and regulation," *Annual Review of Biophysics and Biomolecular Structure*, vol. 27, pp. 133–164, 1998.

[29] C. C. Chung, P. A. Kanetsky, Z. Wang et al., "Meta-analysis identifies four new loci associated with testicular germ cell tumor," *Nature Genetics*, vol. 45, no. 6, pp. 680–685, 2013.

[30] O. A. Andreassen, W. K. Thompson, A. J. Schork et al., "Improved detection of common variants associated with schizophrenia and bipolar disorder using pleiotropy-informed conditional false discovery rate," *PLoS Genetics*, vol. 9, no. 4, Article ID e1003455, 2013.